Electronic Supplementary Material (ESI) for Dalton Transactions.

Impact of Counter Anions on Spin-State Switching of Manganese(III) Complexes Containing Azobenzene Ligand

Subrata Ghosh,[a] *Sukanya Bagchi,*[a] *Sujit Kamilya,*[a] *Sakshi Mehta,*[a] *Debopam Sarkar*,[a] *Radovan Herchel*[b] *and Abhishake Mondal**[,a]

[a]*Solid State and Structural Chemistry Unit, Indian Institute of Science, Sir C V Raman Road, Bangalore 560012, India.*

[b]*Department of Inorganic Chemistry, Faculty of Science, Palacký University, CZ-771 46 Olomouc, Czech Republic.*

[*]Email: mondal@iisc.ac.in

Table of Content:

Experimental Section

Materials and physical measurements

All manipulations were carried out under air unless otherwise stated. Solvents were dried by standard methods and freshly distilled before use. All chemicals were used as purchased from chemical sources without further purification. Azo- salicylaldehyde ligand (Scheme S1) was prepared according to the literature procedure.[1] The crystals of complexes were removed from the mother liquor and dried on filter paper to remove any adhering solvent molecules, before measurement. The elemental analyses of C, H, and N were performed with Thermo Scientific Flash 2000 Organic Elemental Analyzer. Infrared (IR) spectra were recorded in the range of 4000 – 500 cm^{-1} on the Perkin Elmer spectrometer. UV-vis-NIR spectra were carried out in the region of 250 – 2000 nm on a Lambda 750 UV-vis-NIR spectrometer. The UV-vis spectroscopic measurements in solution were performed in quartz cuvettes with a path length of 1 cm. Solid-state measurements were carried out by taking a 5% sample by weight in KBr. Thermogravimetric analysis (TGA) was done on a Mettler Toledo TGA/SDTA851 analyzer with a heating rate of 10 K min^{-1} under a nitrogen atmosphere ranging from 300 K to 573 K. Powder X-ray diffraction (PXRD) measurements were carried out on a PANalytical Empyrean diffractometer at 45 kV and 30 mA, under Cu-Kα radiation (λ = 1.54059 Å). PXRD data analyses were done using PANalytical X'Pert HighScore Plus software.[2] Electrochemistry experiments were performed with a Metrohm Autolab PGSTAT101 using platinum as a working electrode in acetonitrile with 0.2 M ($^{n}Bu_4$)NPF_6 as a supporting electrolyte. Ferrocene was used as an internal reference.

Magnetic Measurements

The magnetic susceptibility measurements were carried out with Quantum Design MPMS-XL EverCool SQUID magnetometer, between 2 and 400 K for dc applied fields ranging from -5 T to 5 T for **1** - **4**. Polycrystalline samples of **1** - **4** (18.32, 21.68, 9.50, and 32.06 mg, respectively) were introduced in a polyethylene bag (2.8 × 0.75 × 0.02 cm) and were subjected to measurements. The

temperature-dependent data were measured using 1000 Oe and 10000 Oe dc fields. The isothermal magnetization data were acquired at 1.9, 5, 6, and 8 K. *M vs H* measurements were performed at 100 K to check for the presence of ferromagnetic or diamagnetic impurities which were found to be absent. The magnetic data were corrected for the sample holder and the diamagnetic contribution. The *ac* susceptibility measurements were measured with an oscillating *ac* field of 3 Oe with frequency between 1 to 1500 Hz.

X-ray crystallography

Single−crystal X−ray structure diffraction studies of complexes **1** - **4** were performed with a Bruker SMART APEX CCD diffractometer equipped with graphite−monochromated Mo Kα radiation (λ = 0.71073 Å). The single crystal was mounted on a crystal mounting loop with the help of Paratone oil at 240 K and slowly cooled down to the measured temperature with a 2 K/min ramping rate using a liquid nitrogen gas-stream cooling device, followed by data collection at respective temperatures. Data integration and reduction were carried out using SAINT software, and empirical absorption corrections were performed using the SADABS program.[3] Structures were solved using direct methods and refined with a full-matrix least-squares method on F^2 using SHELXL-2018 included in WinGX programs suite[4] and OLEX 2 version 1.3.0.[5] The packing diagrams were made using Mercury 4.2.0.[6] Complex **2** contains severely disordered one CH_3CN molecule, which was treated by using SOLVENT MASK procedure in OLEX 2 which is equivalent to SQUEEZE in PLATON. Details of SOLVENT MASK procedure and corresponding results are provided in the respective CIF file.

All other non-hydrogen atoms of complexes **1** - **4** were refined anisotropically and hydrogen atoms were labeled to ideal positions and refined isotropically using a riding model. CCDC 2098342, 2098344, 2098402, 2098404, and 2098406 contain the supplementary crystallographic

data for this paper. These data can be obtained free of charge from The Cambridge Crystallographic Data Centre via www.ccdc.cam.ac.uk/data_request/cif.

Scheme

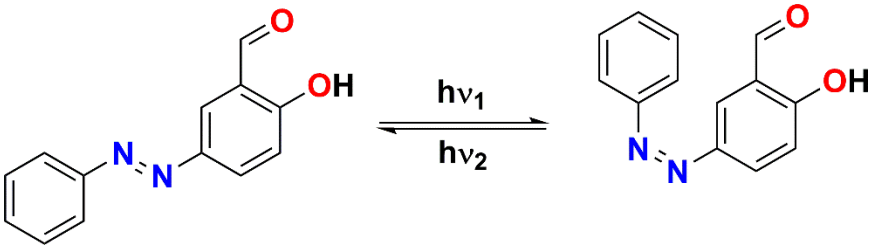

Scheme S1. Schematic presentation of photoisomerization of azo-salicylaldehyde.

Figures

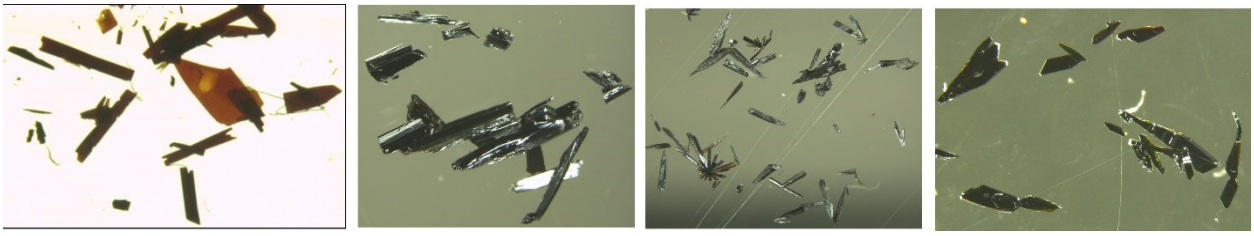

Fig. S1. Crystal images for complexes **1** – **4** (left to right).

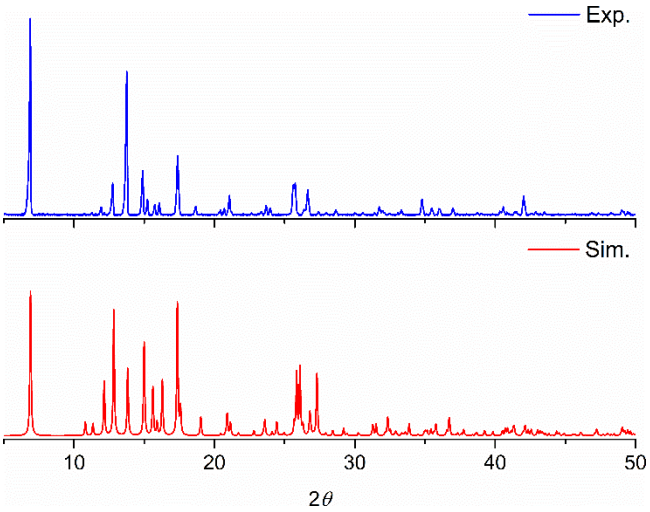

Fig. S2. Comparison of the room temperature experimental PXRD pattern and the 100 K simulated pattern for **1**.

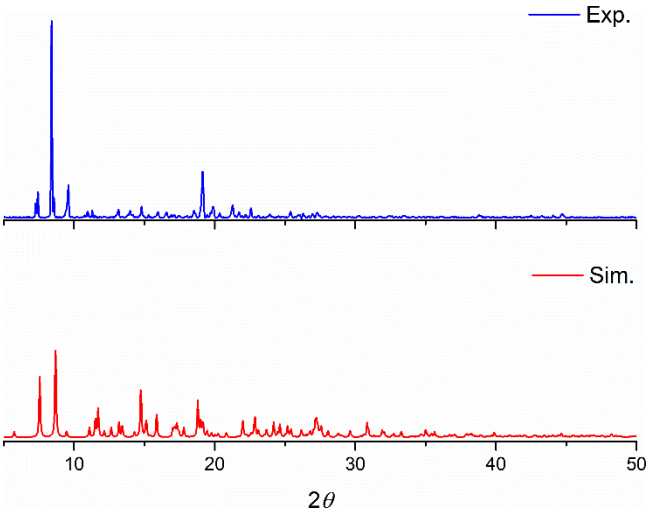

Fig. S3. Comparison of the room temperature experimental PXRD pattern and the 100 K simulated pattern for **2**.

The reason for the slight deviation in the experimental PXRD data for **2** is probably due to the partial solvent loss during the sample preparation for the PXRD measurement at room temperature.

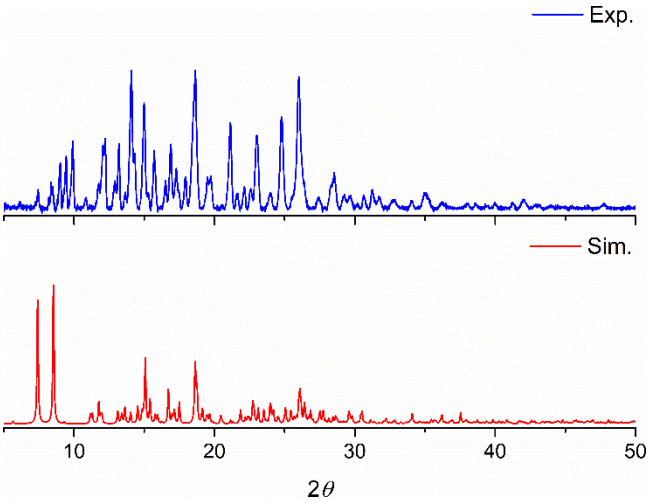

Fig. S4. Comparison of the room temperature experimental PXRD pattern and the 100 K simulated pattern for **3**.

The reason for the slight deviation in the experimental PXRD data for **3** is probably due to the partial solvent loss during the sample preparation for the PXRD measurement at room temperature.

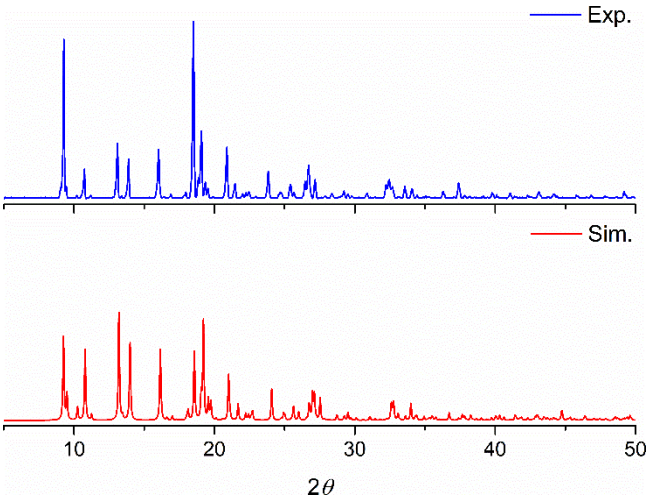

Fig. S5. Comparison of the room temperature experimental PXRD pattern and the 100 K simulated pattern for **4**.

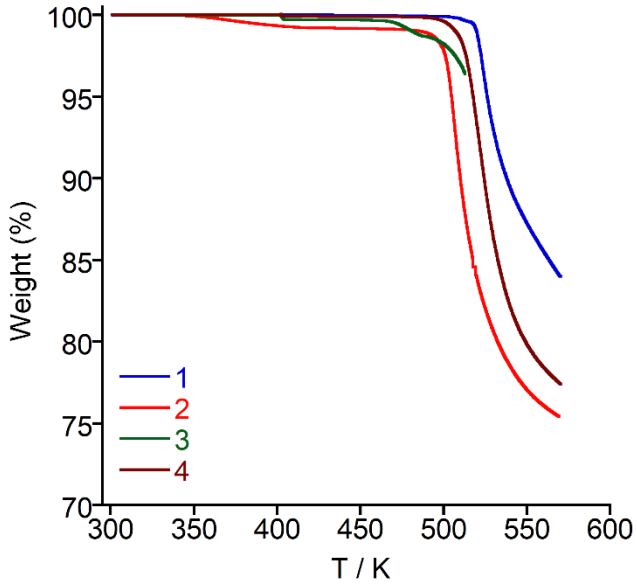

Fig. S6. TGA curves for **1 – 4** from 300 K to 573 K temperature range at 10 K min^{-1} sweep rate under N_2 atmosphere.

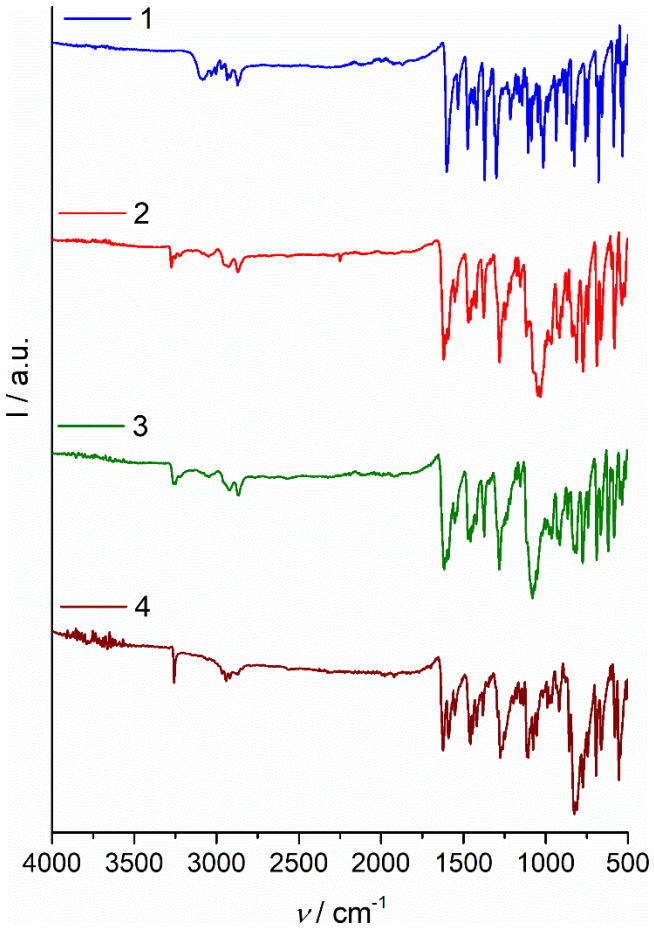

Fig. S7. ATR IR spectra of **1** – **4** at room temperature.

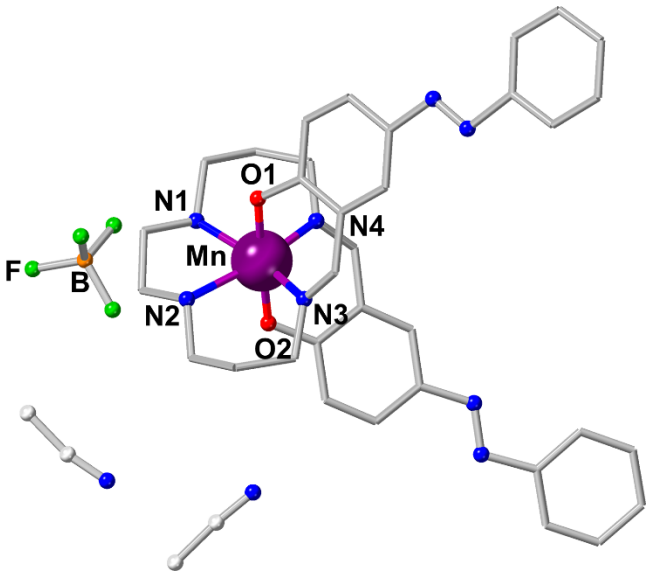

Fig. S8. Perspective view of complex **2** at 100 K. Hydrogen atoms are omitted for clarity (Mn: Purple, C: gray, N: blue, O: red, B: orange, F: light-green).

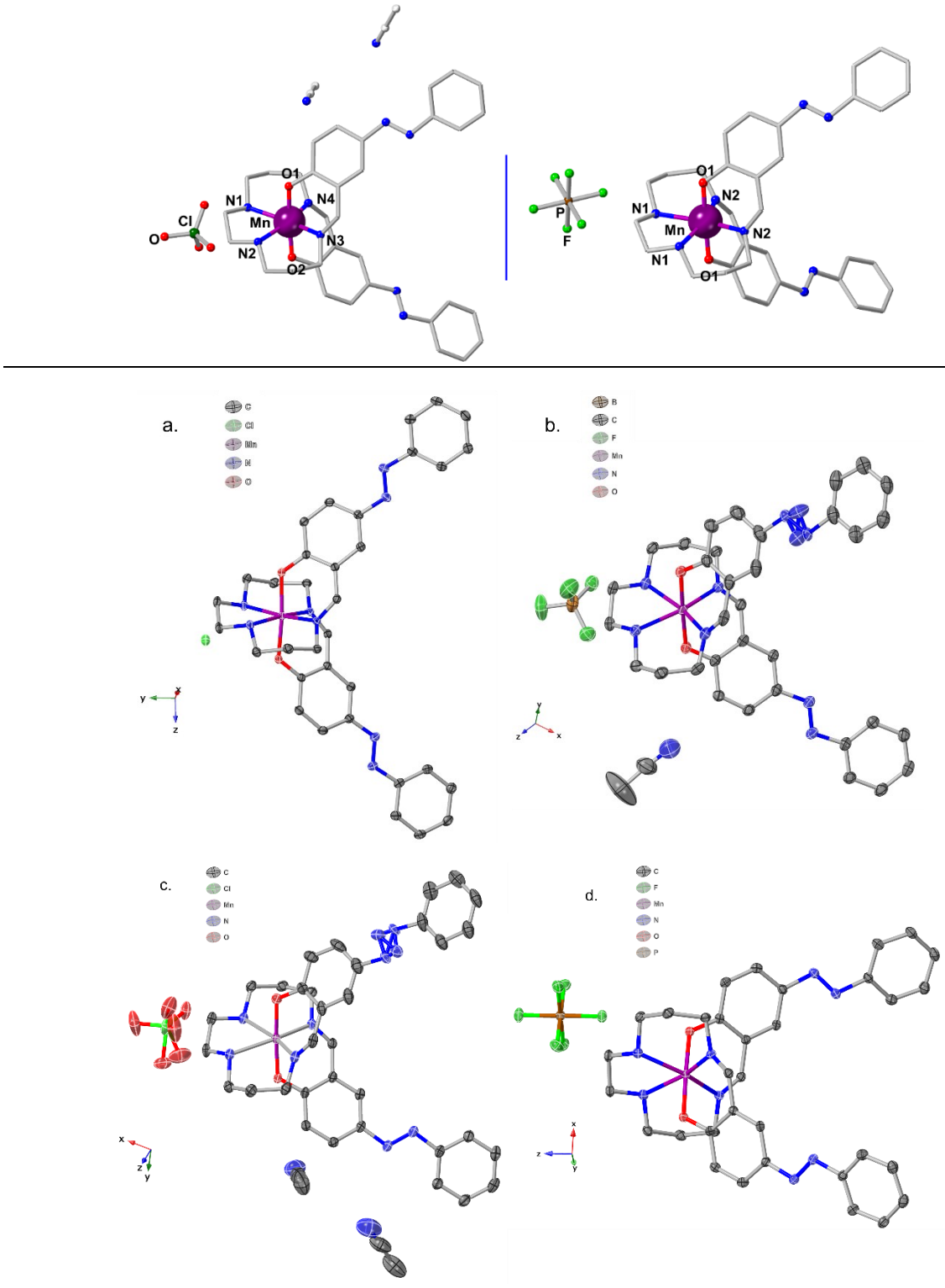

Fig. S9. Top: Perspective view of complexes **3** (left) and **4** (right) at 100 K. Hydrogen atoms are omitted for clarity (Mn: Purple, C: gray, N: blue, O: red, F: light-green, P: brown, Cl: green); Bottom: Perspective view of complex **1**(a), **2**(b), **3**(c) and **4**(d) showing anisotropic displacement parameter at 100 K.

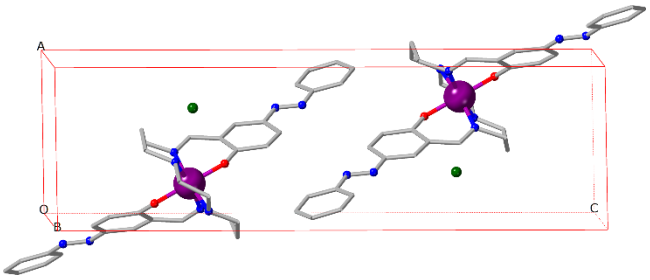

Fig. S10. Perspective view of the unit cell in **1** at 100 K. Hydrogen atoms are omitted for clarity (Mn: Purple, C: gray, N: blue, O: red, Cl: green).

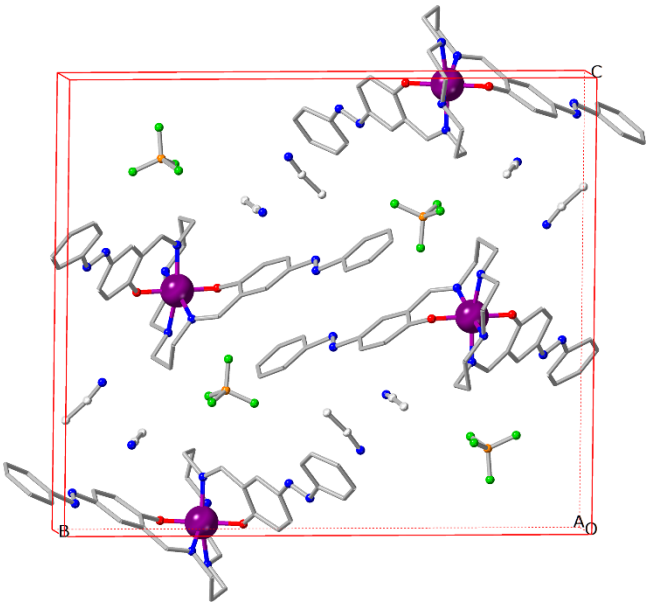

Fig. S11. Perspective view of the unit cell in **2** at 100 K. Hydrogen atoms are omitted for clarity (Mn: Purple, C: gray, N: blue, O: red, B: orange, F: light-green).

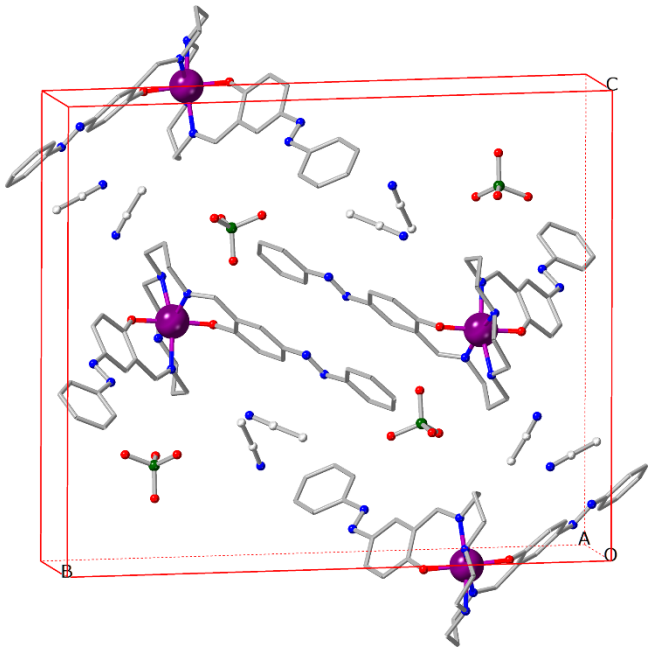

Fig. S12. Perspective view of the unit cell in **3** at 100 K. Hydrogen atoms are omitted for clarity (Mn: Purple, C: gray, N: blue, O: red, Cl: green).

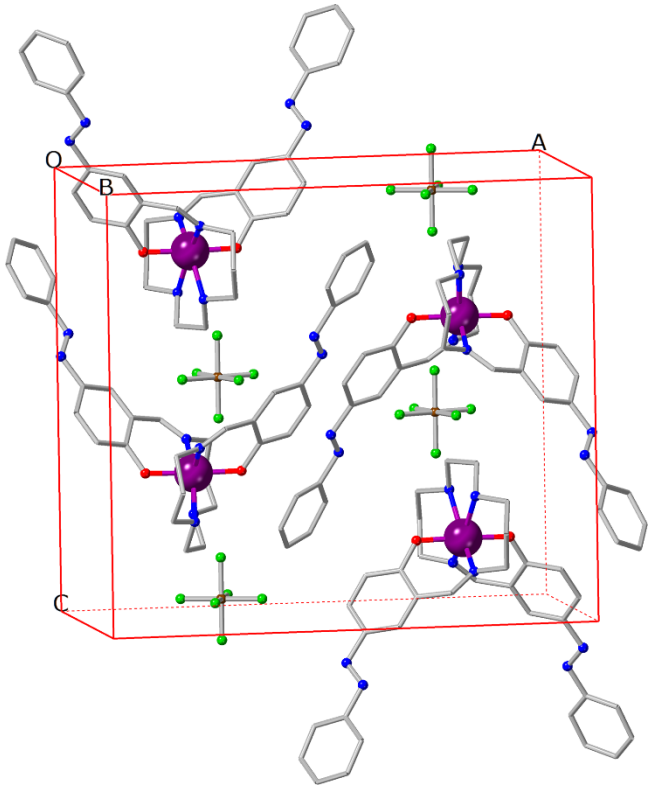

Fig. S13. Perspective view of the unit cell in **4** at 100 K. Hydrogen atoms are omitted for clarity (Mn: Purple, C: gray, N: blue, O: red, P: brown, F: light-green).

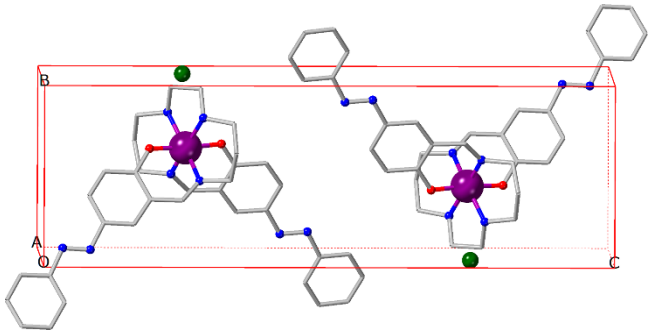

Fig. S14. Perspective view of the unit cell in **1** at 240 K. Hydrogen atoms are omitted for clarity (Mn: Purple, C: gray, N: blue, O: red, Cl: green).

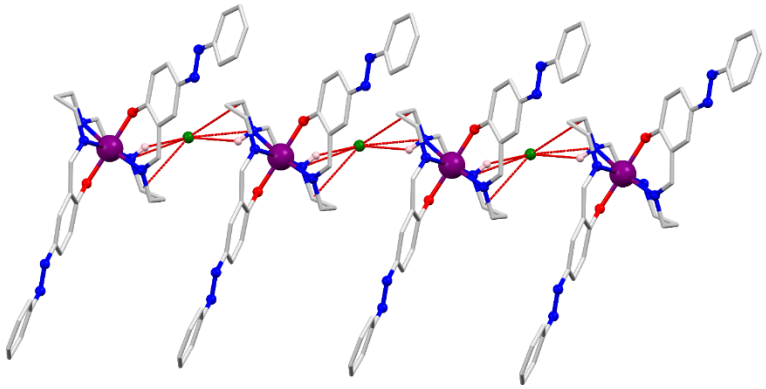

Fig. S15. View of N–H···Cl and C···Cl interactions (red lines) forming a 1D chain in **1** at 240 K

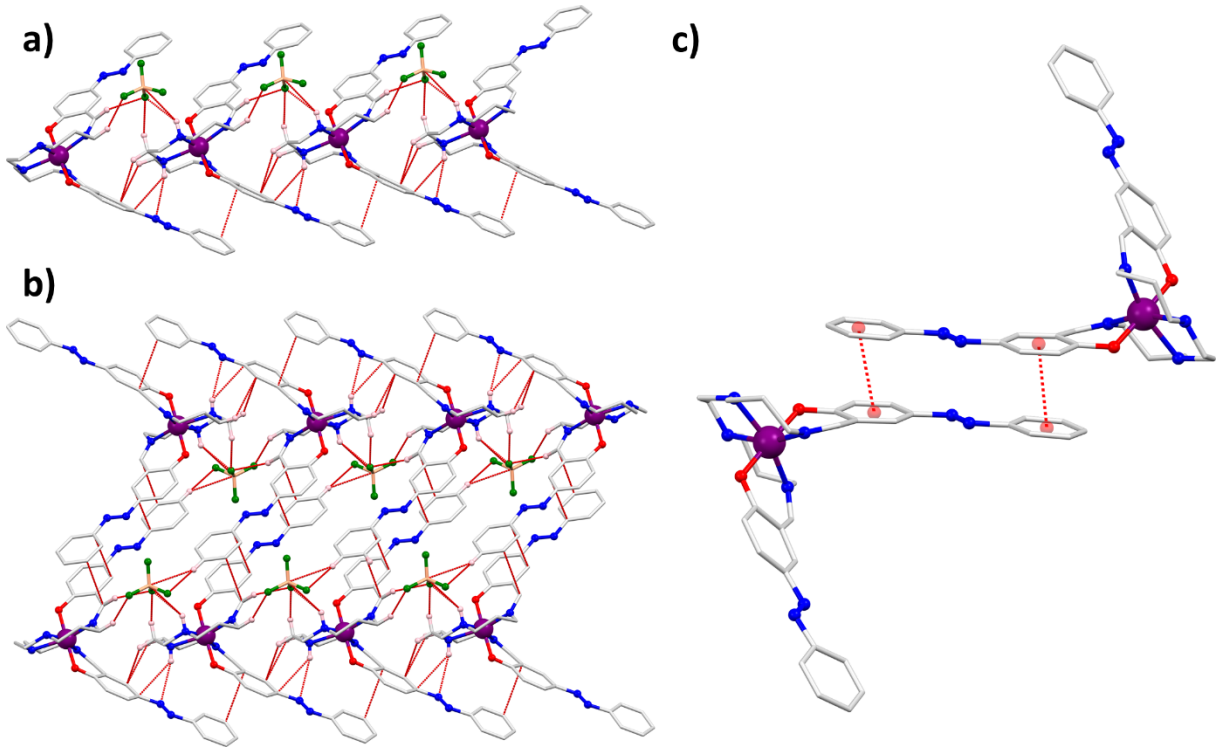

Fig. S16. View of N–H···F interactions (red lines) forming a 1D chain (a), formation of the 2D supramolecular structure via C–H···F interactions (red lines) (b), and view of $\pi\cdots\pi$ interactions (red lines) (c) in **2** at 100 K.

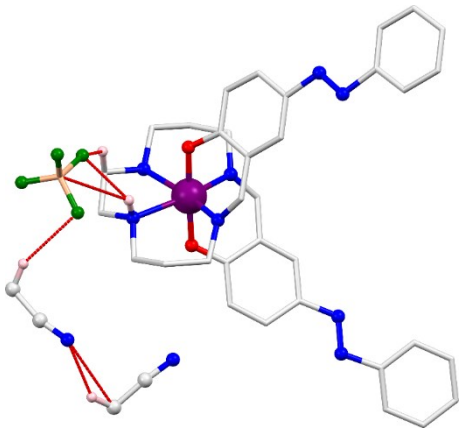

Fig. S17. Perspective view of supramolecular weak interactions among monocationic unit, counter anion, and solvent molecules (red lines) in **2** at 100 K.

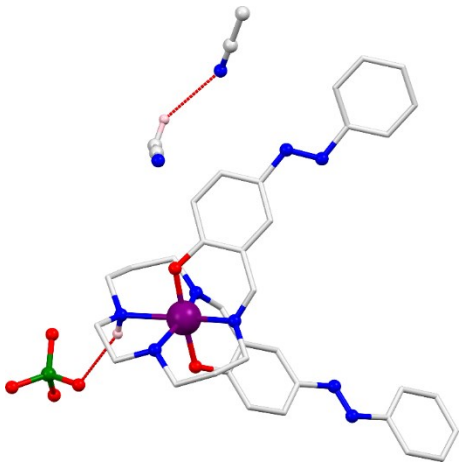

Fig. S18. Perspective view of supramolecular weak interactions among monocationic unit, counter anion, and solvent molecules (red lines) in **3** at 100 K.

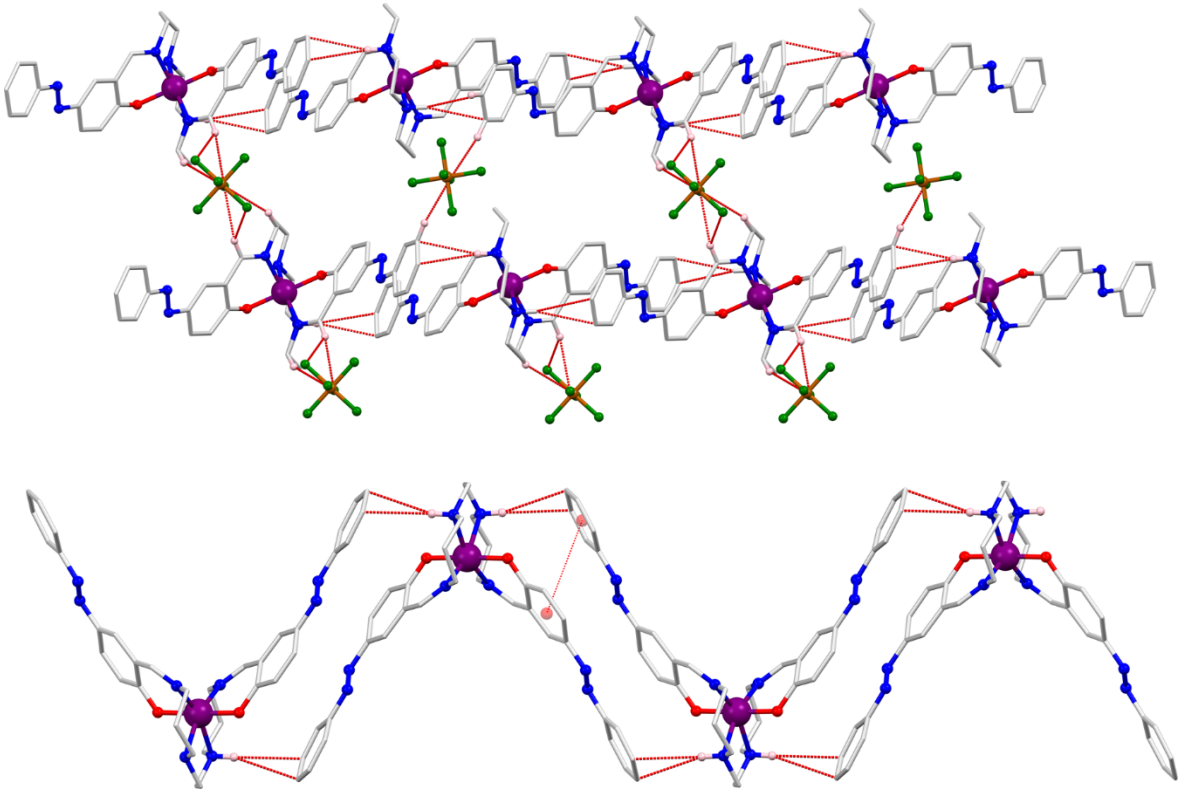

Fig. S19. View of C–H···F interactions (red lines) forming a 2D supramolecular chain (top), and C–H···F and $\pi\cdots\pi$ interactions (red lines) in the 1D chain (bottom) in **4** at 100 K.

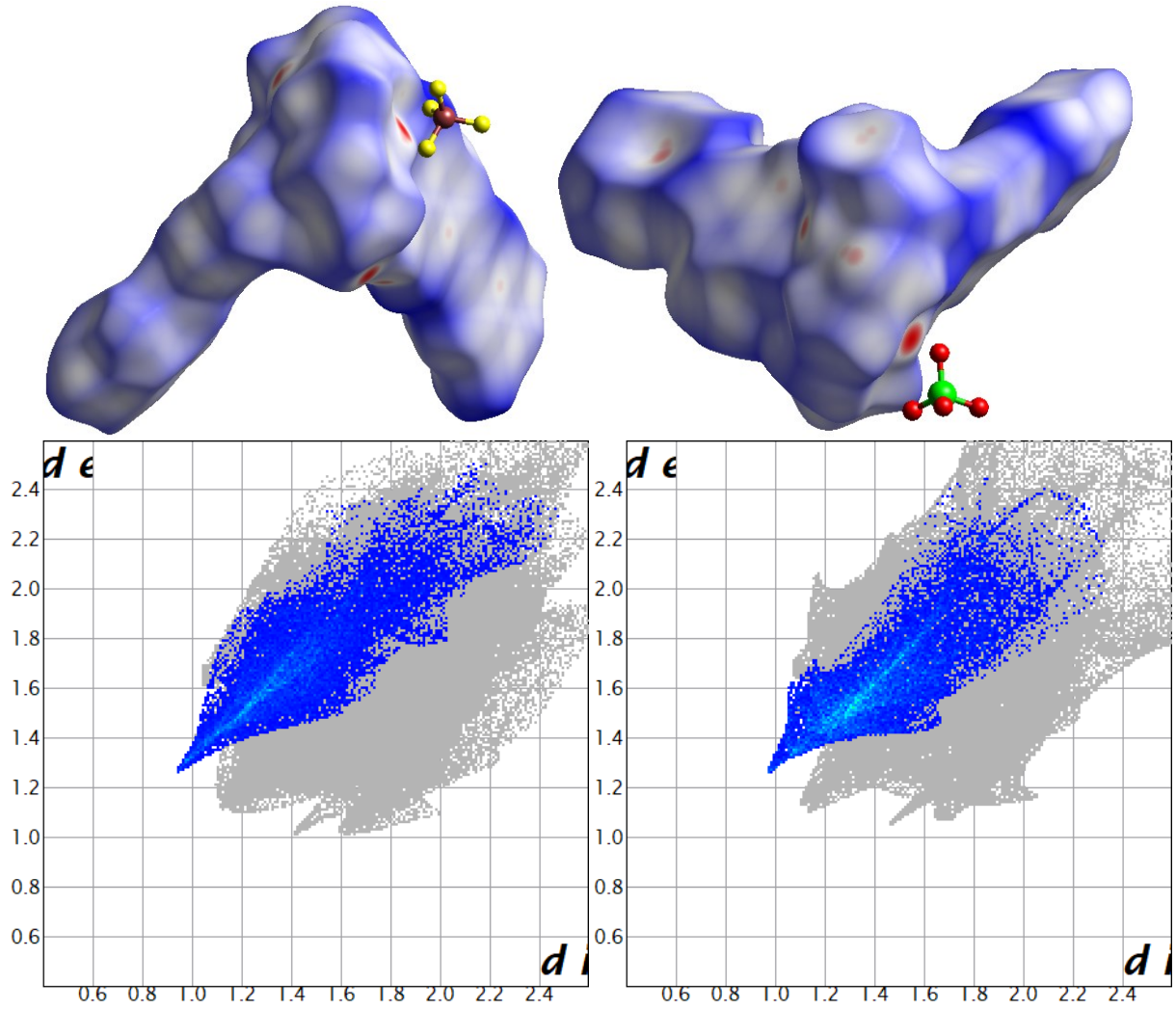

Fig. S20. Hirshfeld surface analysis of complexes **2** and **3**, showing the d_{norm} surfaces of the monocationic unit ([Mn(5azo-sal$_2$-323)]$^+$) (top) and 2D fingerprint plots of all contacts: F···H (11.0%) for **2** (bottom, left) and O···H (11.5) for **3** (bottom, right) at 100 K.

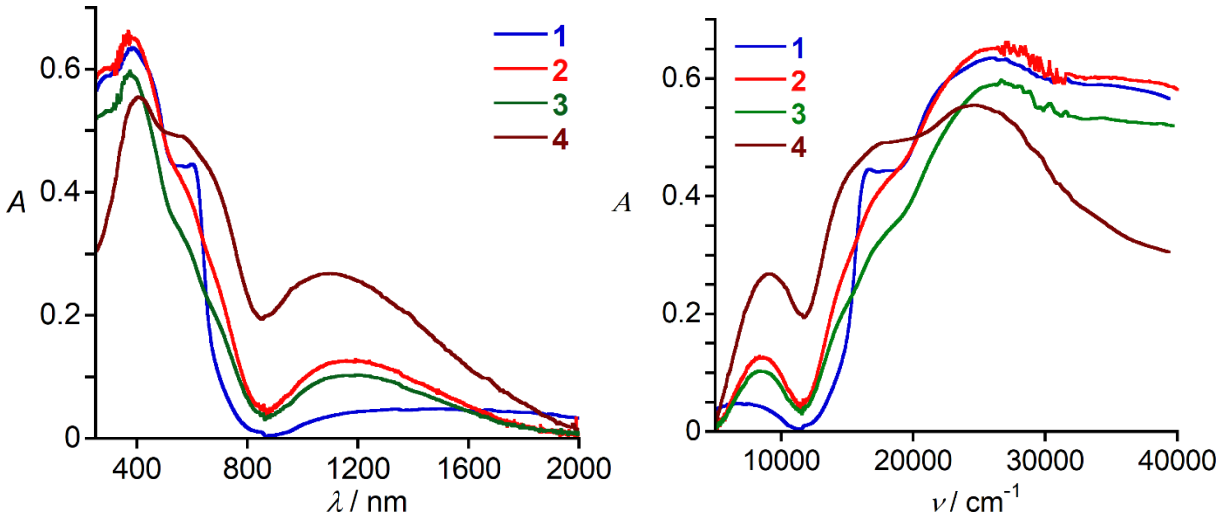

Fig. S21. Solid-state UV-vis-NIR spectra of **1** – **4** in KBr at room temperature (left: wavelength scale and right: wavenumber scale).

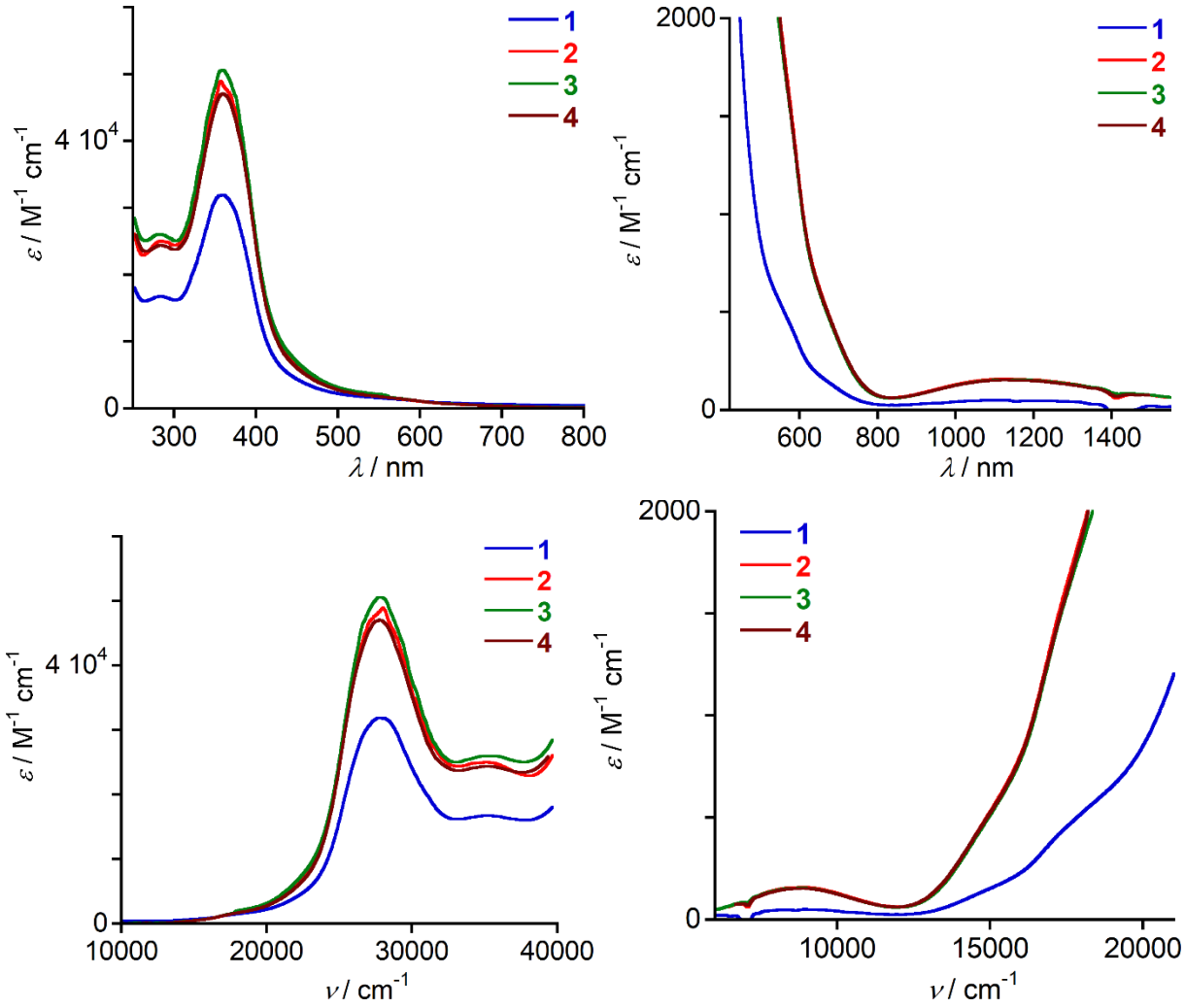

Fig. S22. UV-vis-NIR spectra of **1** – **4** in MeCN with dilute (left) and concentrated (right) solutions at room temperature (top: wavelength scale and bottom: wavenumber scale).

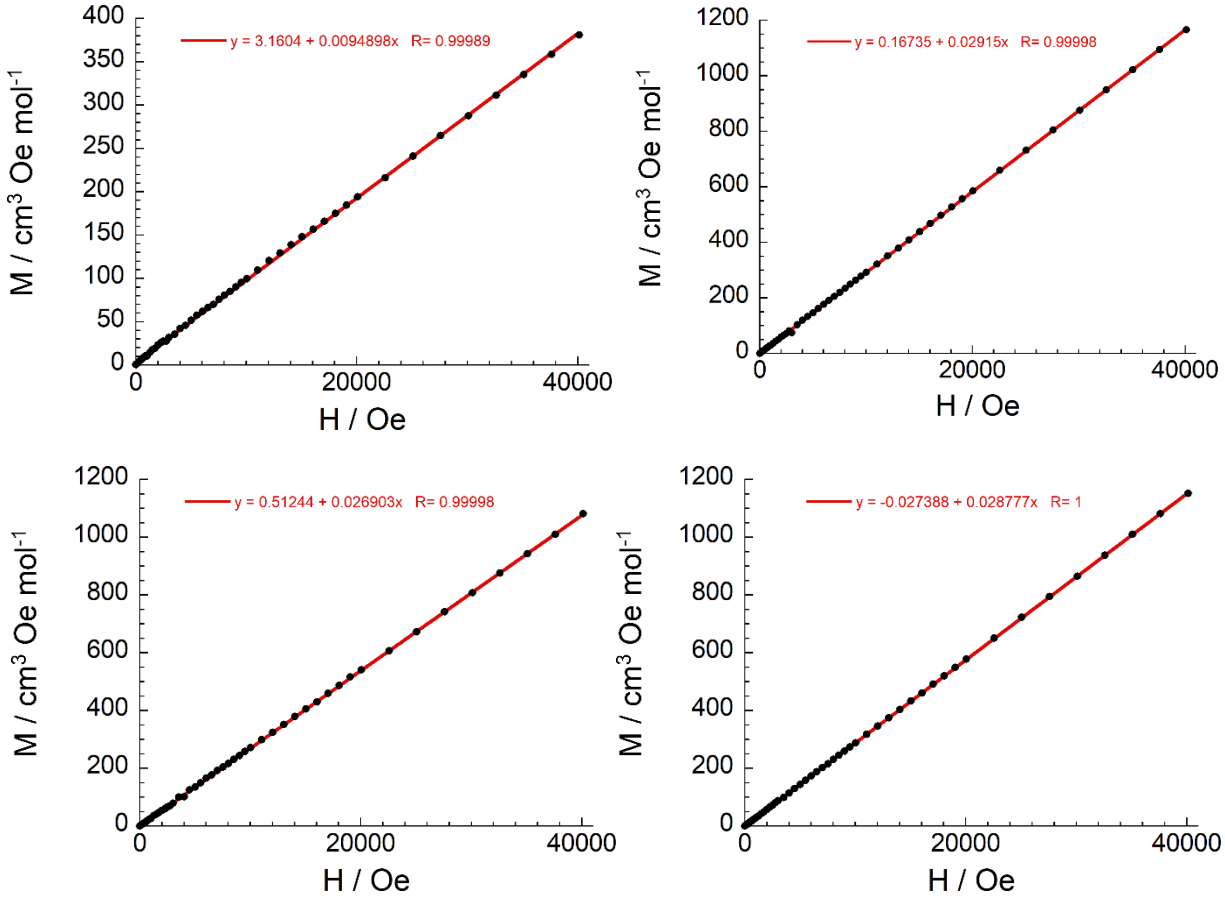

Fig. S23. Field dependence of the magnetization as *M vs H* plots for **1** (Top, left), **2** (top, right), **3** (bottom, left), and **4** (bottom, right) at 100 K. The solid line is the best fit.

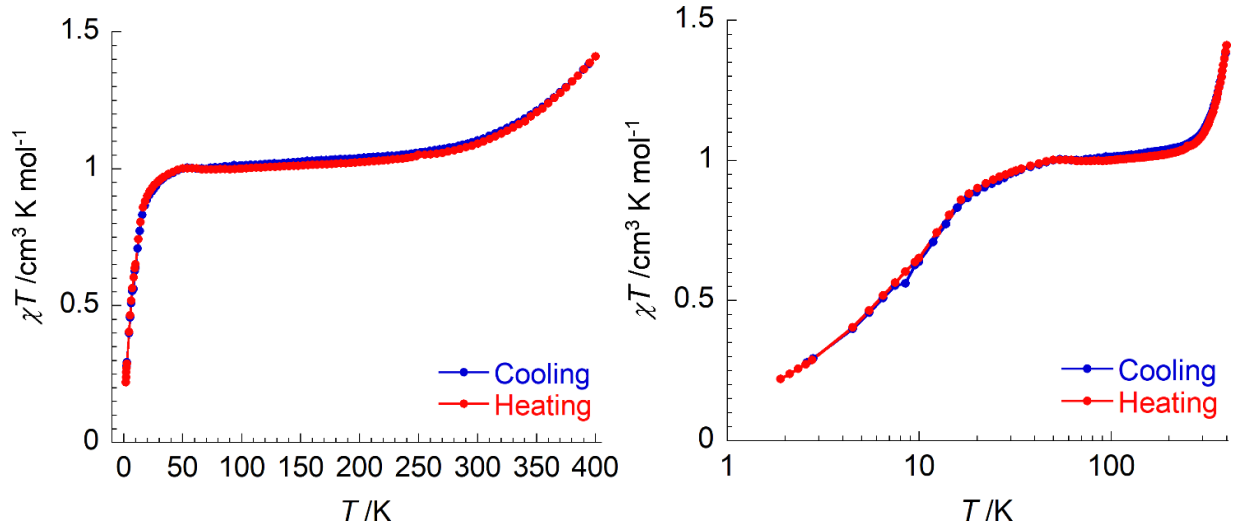

Fig. S24. Temperature dependence of χT product for **1** at 10000 Oe in cooling and heating mode. Left: in normal scale; Right: in log scale.

The following equation deduced from the ideal solution model was applied to fit the spin crossover properties observed by magnetic studies.

$$X = X_{LS} + \frac{X_{HS} - X_{LS}}{1 + \exp\left[\Delta H/R\ (1/T - 1/T_{1/2})\right]}$$

X = χT product

X_{LS} = χT product for pure low-spin

X_{HS} = χT product for pure high-spin

ΔH = Enthalpy change associated with the spin crossover phenomenon

R = Ideal gas constant

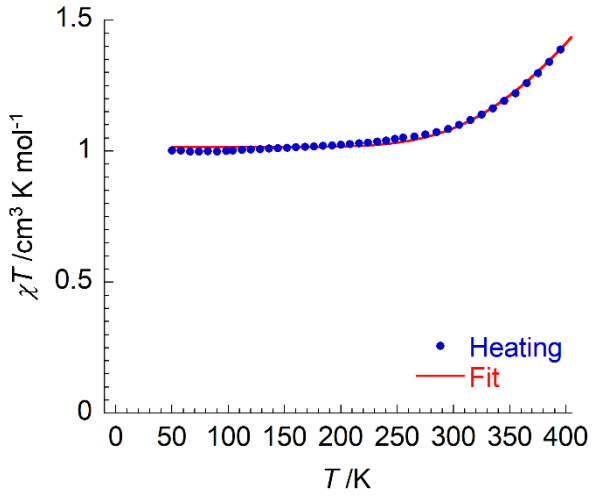

Fig. S25. χT *vs.* T data fit of **1** using the ideal solution model.

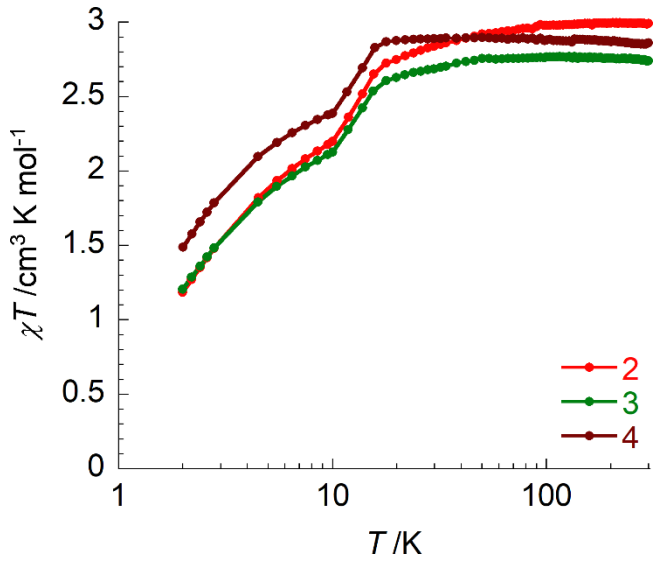

Fig. S26. Temperature dependence of χT product in log scale for **2** – **4** at 1000 Oe.

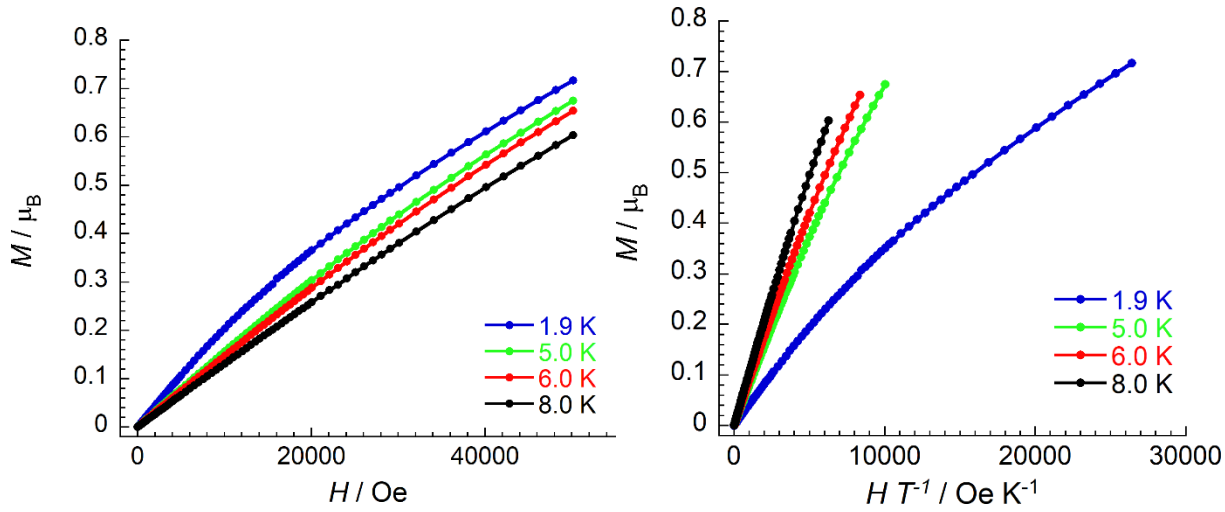

Fig. S27. Field dependence of the magnetization as *M* vs *H* (left) and *M* vs *H/T* (right) plots for **1** at 1.9, 5, 6, and 8 K. The solid lines are a guide for the eyes.

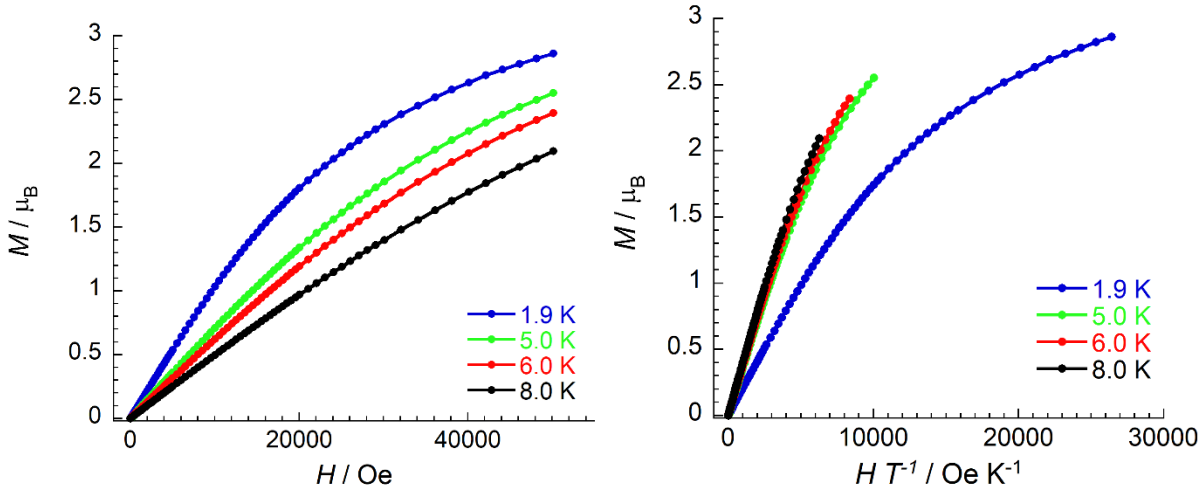

Fig. S28. Field dependence of the magnetization as *M* vs *H* (left) and *M* vs *H/T* (right) plots for **2** at 1.9, 5, 6, and 8 K. The solid lines are a guide for the eyes.

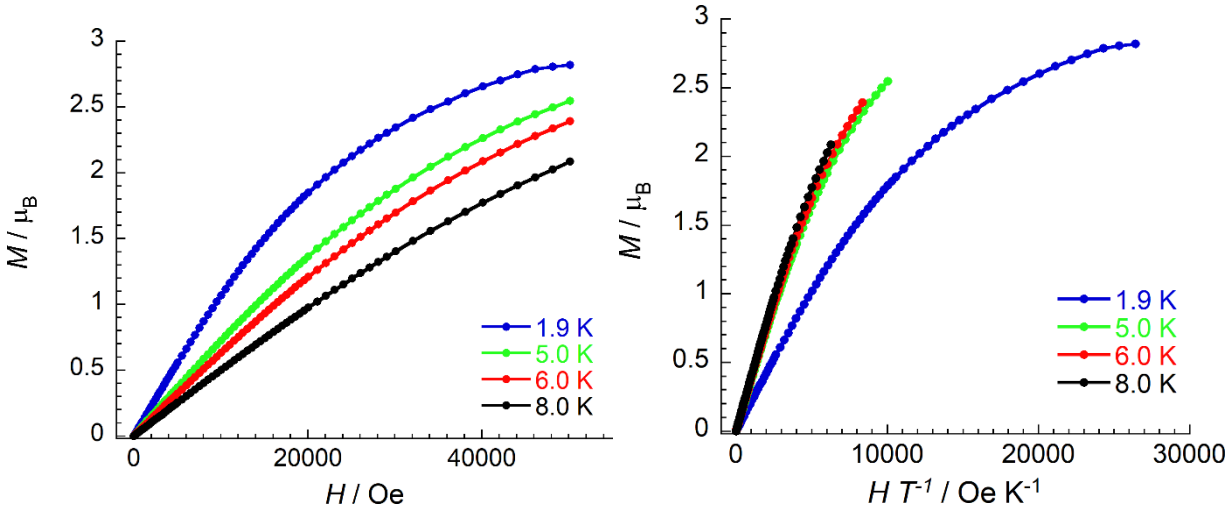

Fig. S29. Field dependence of the magnetization as *M* vs *H* (left) and *M* vs *H/T* (right) plots for **3** at 1.9, 5, 6, and 8 K. The solid lines are a guide for the eyes.

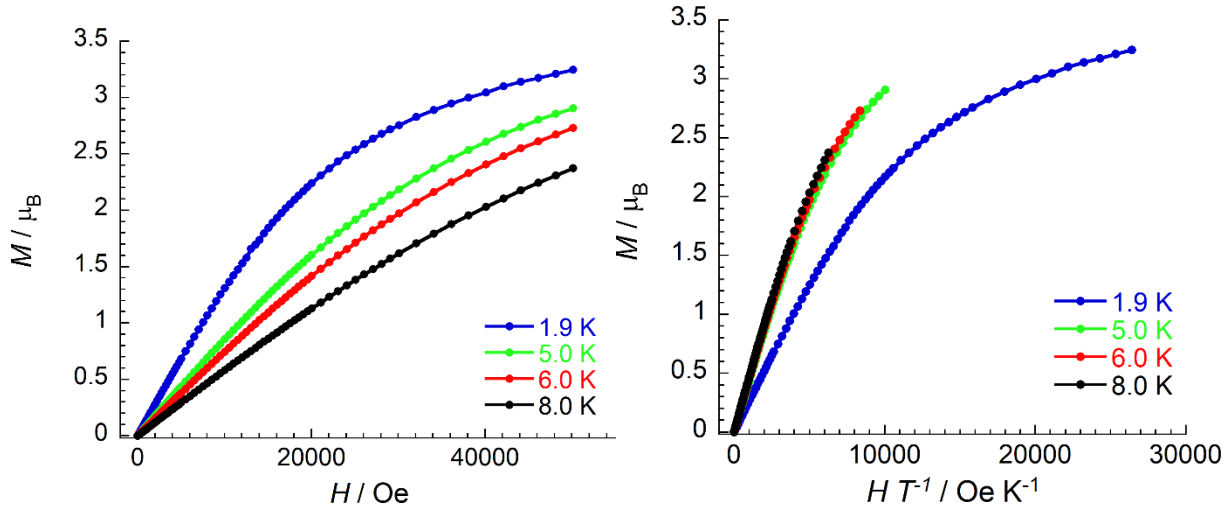

Fig. S30. Field dependence of the magnetization as *M* vs *H* (left) and *M* vs *H/T* (right) plots for **4** at 1.9, 5, 6, and 8 K. The solid lines are a guide for the eyes.

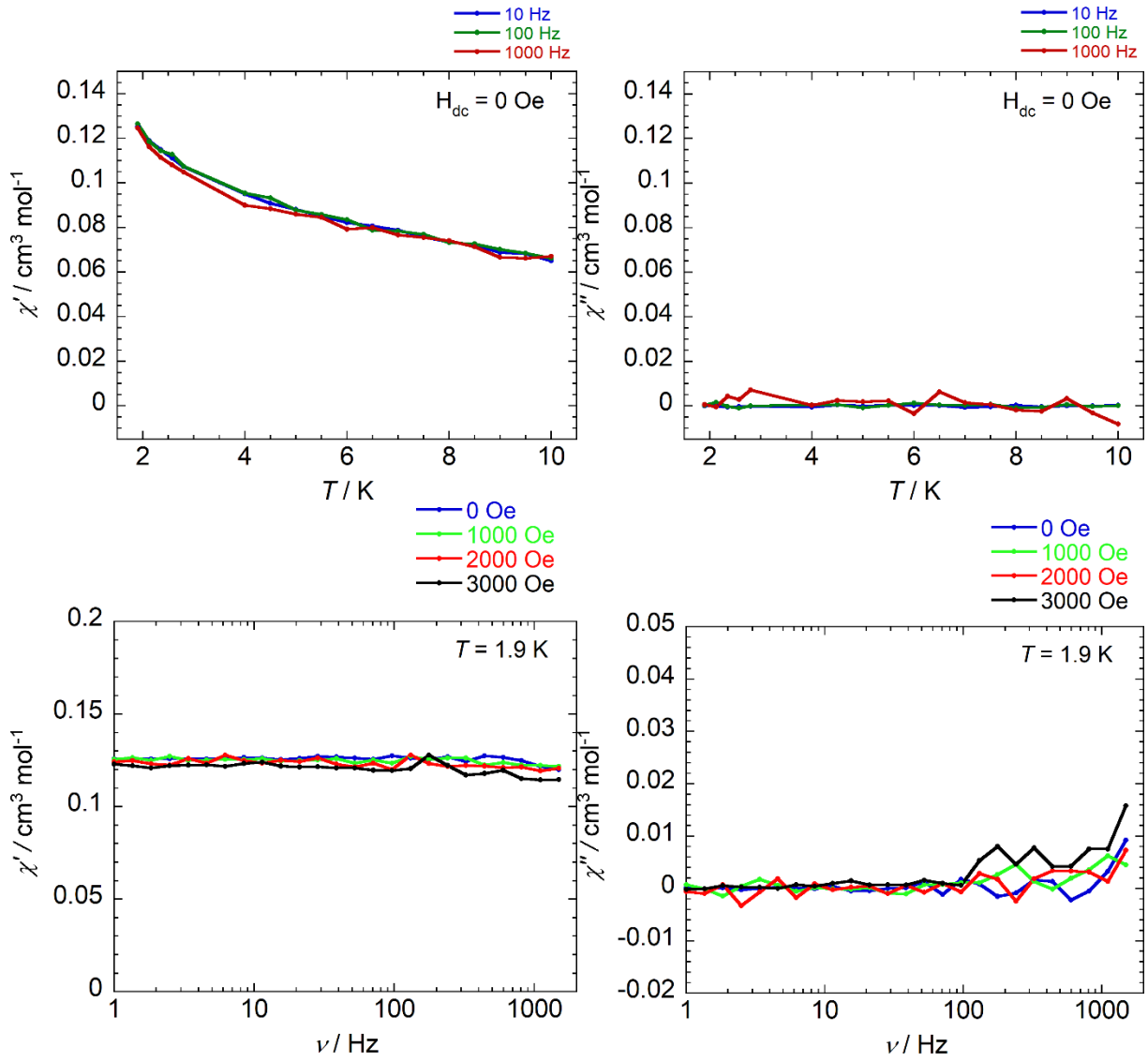

Fig. S31. Frequency vs temperature plot of the real (χ', left) and imaginary (χ'', right) components of the ac susceptibility at 0 Oe external dc field and different temperatures from 1.9 – 15 K (top) and different external dc field at 1.9 K (bottom), respectively with a 3 Oe ac field for a polycrystalline sample of **1**.

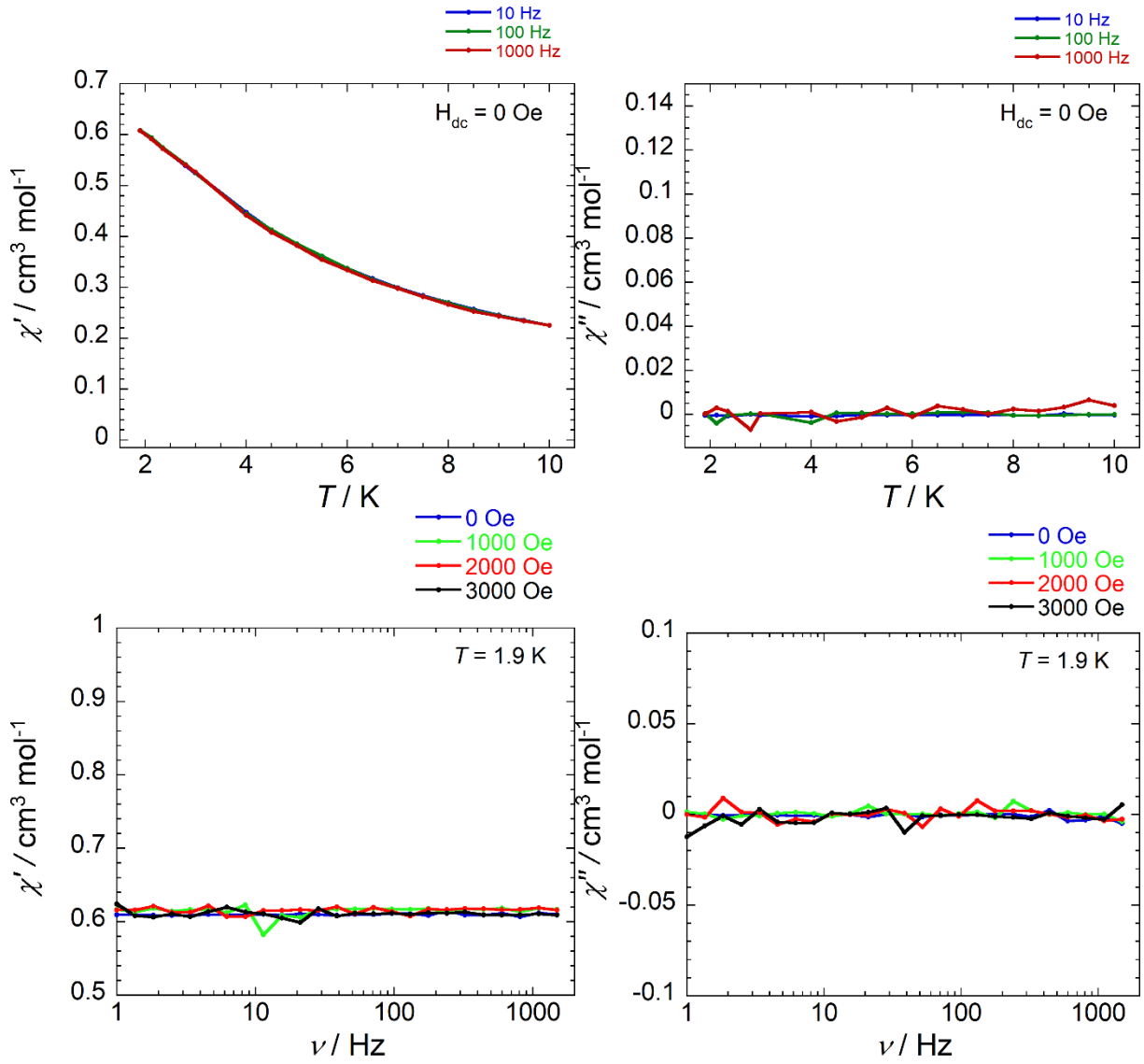

Fig. S32. Frequency vs temperature plot of the real (χ', left) and imaginary (χ'', right) components of the ac susceptibility at 0 Oe external dc field and different temperatures from 1.9 – 15 K (top) and different external dc field at 1.9 K (bottom), respectively with a 3 Oe ac field for a polycrystalline sample of **2**.

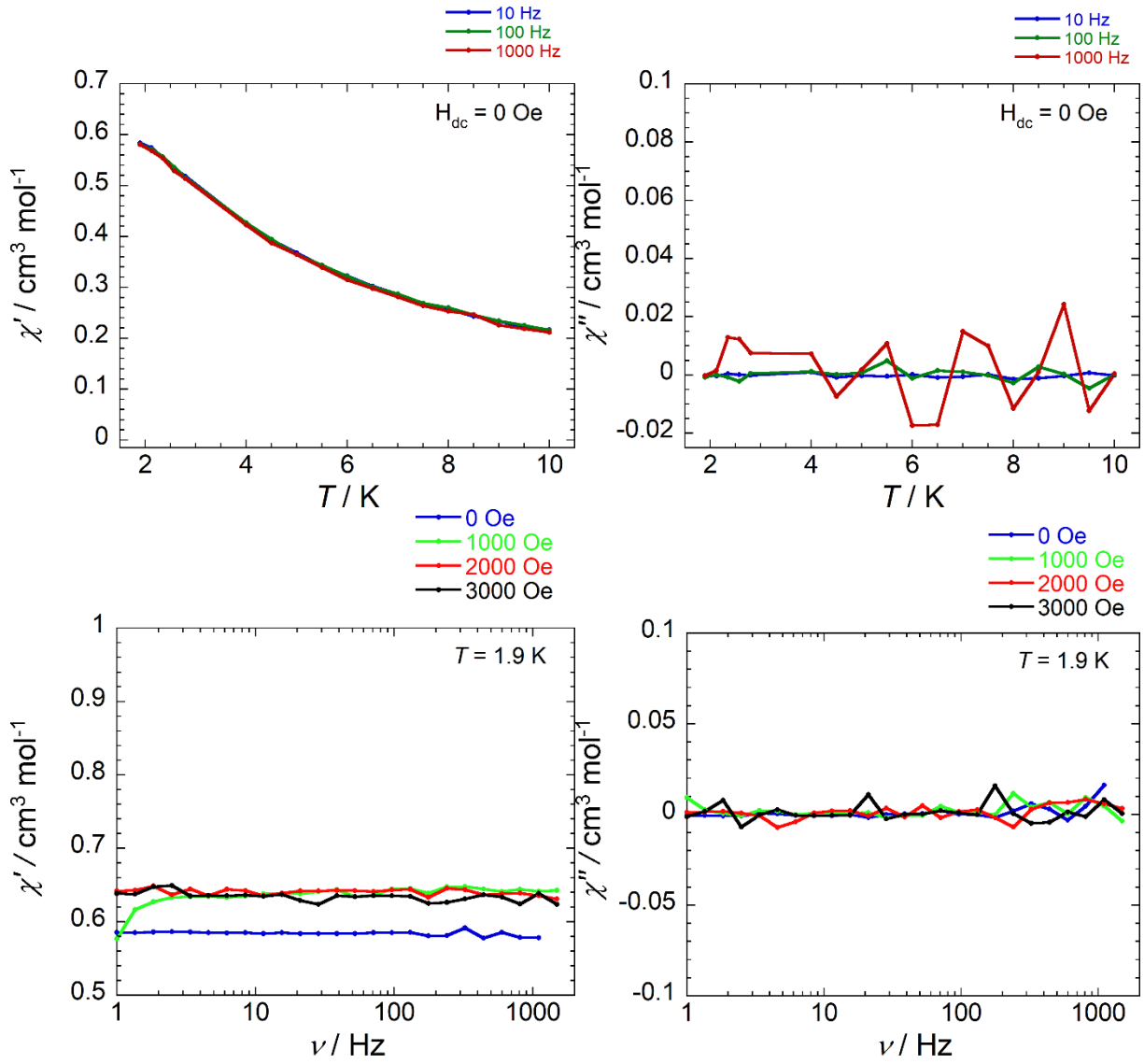

Fig. S33. Frequency vs temperature plot of the real (χ', left) and imaginary (χ'', right) components of the ac susceptibility at 0 Oe external dc field and different temperatures from 1.9 – 15 K (top) and different external dc field at 1.9 K (bottom), respectively with a 3 Oe ac field for a polycrystalline sample of **3**.

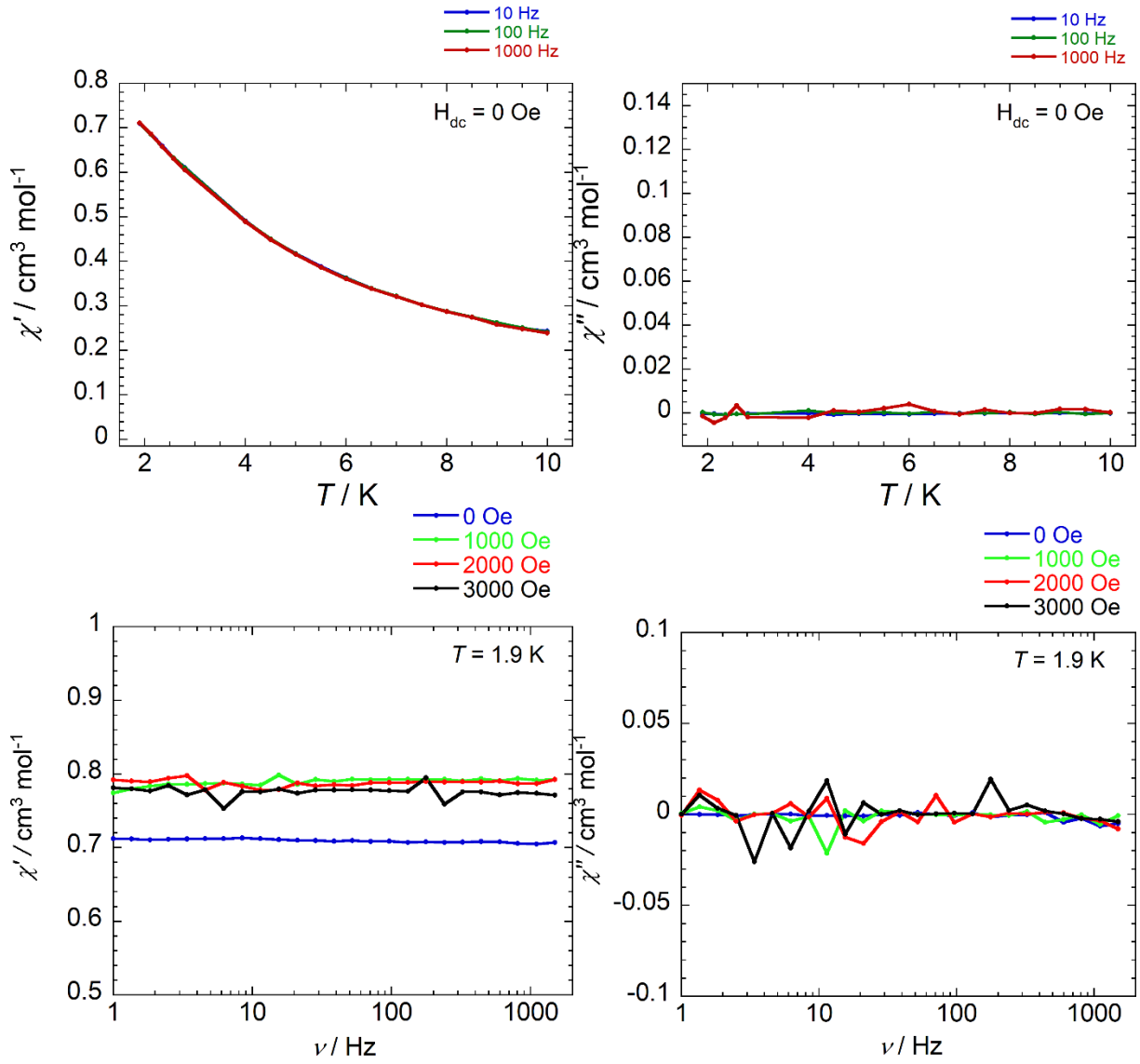

Fig. S34. Frequency vs temperature plot of the real (χ', left) and imaginary (χ'', right) components of the ac susceptibility at 0 Oe external dc field and different temperatures from 1.9 – 15 K (top) and different external dc field at 1.9 K (bottom), respectively with a 3 Oe ac field for a polycrystalline sample of **4**.

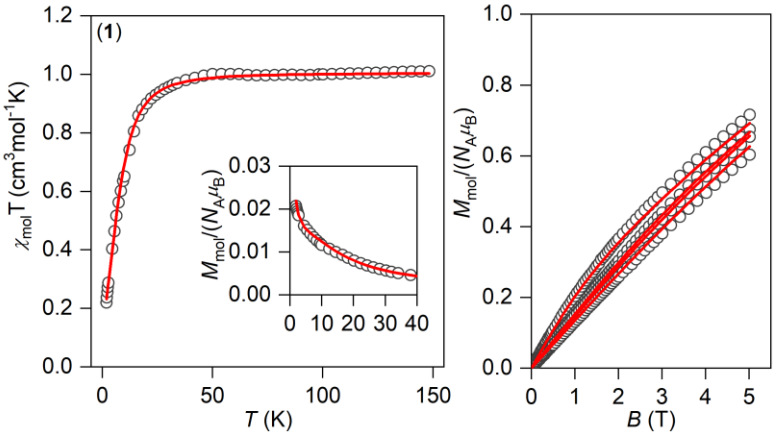

Fig. S35. Left: Temperature dependence of χT product for **1**. Field dependence of the magnetization as M vs B plot of **1** at 1.9, 5, 6, and 8 K. The empty symbols – experimental data, full lines – calculated data with parameters in text.

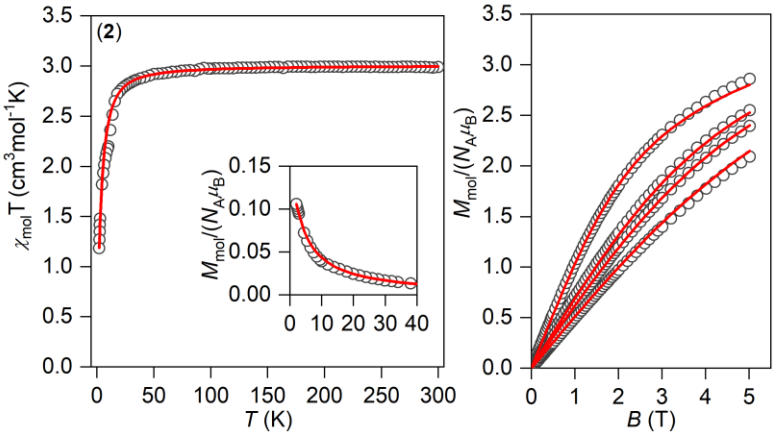

Fig. S36. Left: Temperature dependence of χT product for **2**. Field dependence of the magnetization as M vs B plot of **2** at 1.9, 5, 6, and 8 K. The empty symbols – experimental data, full lines – calculated data with parameters in text.

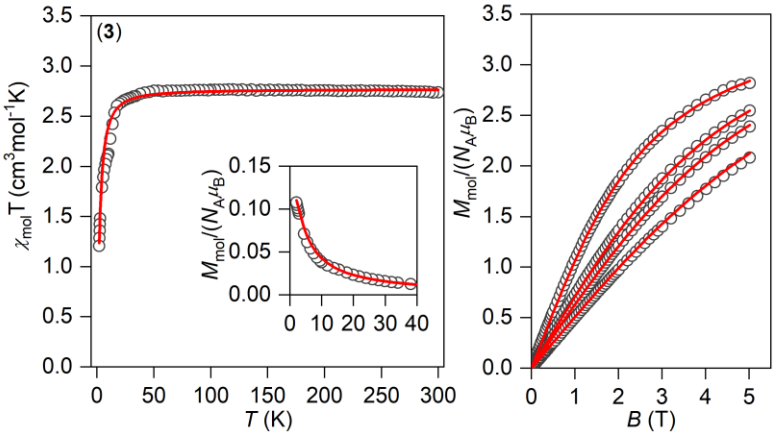

Fig. S37. Left: Temperature dependence of χT product for **3**. Field dependence of the magnetization as M vs B plot of **3** at 1.9, 5, 6, and 8 K. The empty symbols – experimental data, full lines – calculated data with parameters in text.

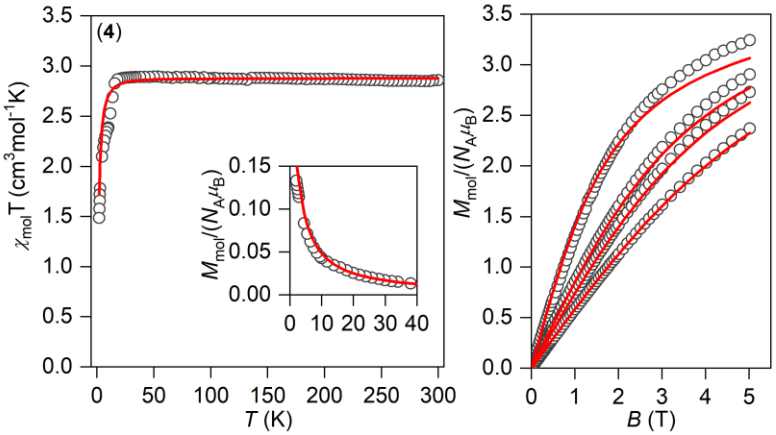

Fig. S38. Left: Temperature dependence of χT product for **4**. Field dependence of the magnetization as M vs B plot of **4** at 1.9, 5, 6, and 8 K. The empty symbols – experimental data, full lines – calculated data with parameters in text.

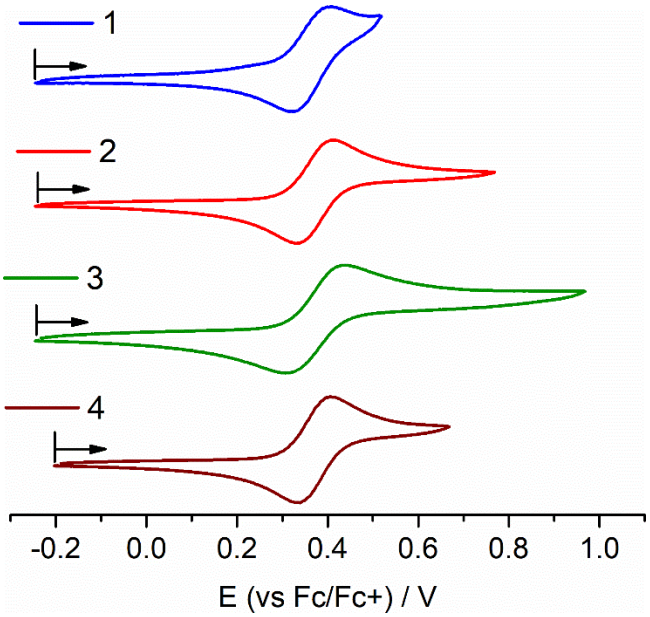

Fig. S39. Cyclic voltammograms for reduction of **1** – **4** in 0.2 M (^{n}Bu$_4$N)PF$_6$ / MeCN with a scan rate of 100 mV s^{-1}. Arrow indicates the open circuit potential with the direction of the potential sweep.

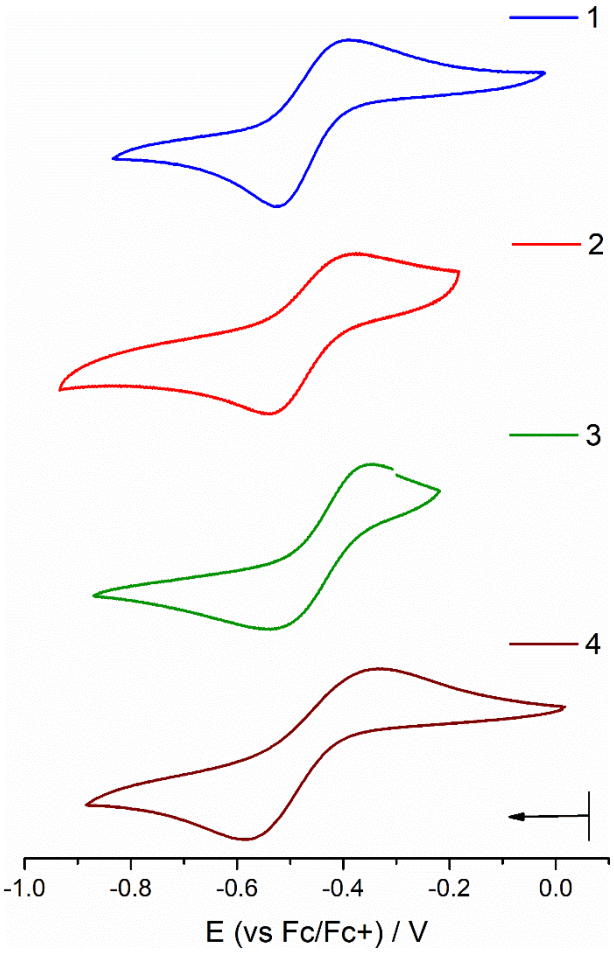

Fig. S40. Cyclic voltammograms for reduction of **1** – **4** in 0.2 M (^{n}Bu$_4$N)PF$_6$ / MeCN with a scan rate of 100 mV s^{-1}. Arrow indicates the open circuit potential with the direction of the potential sweep.

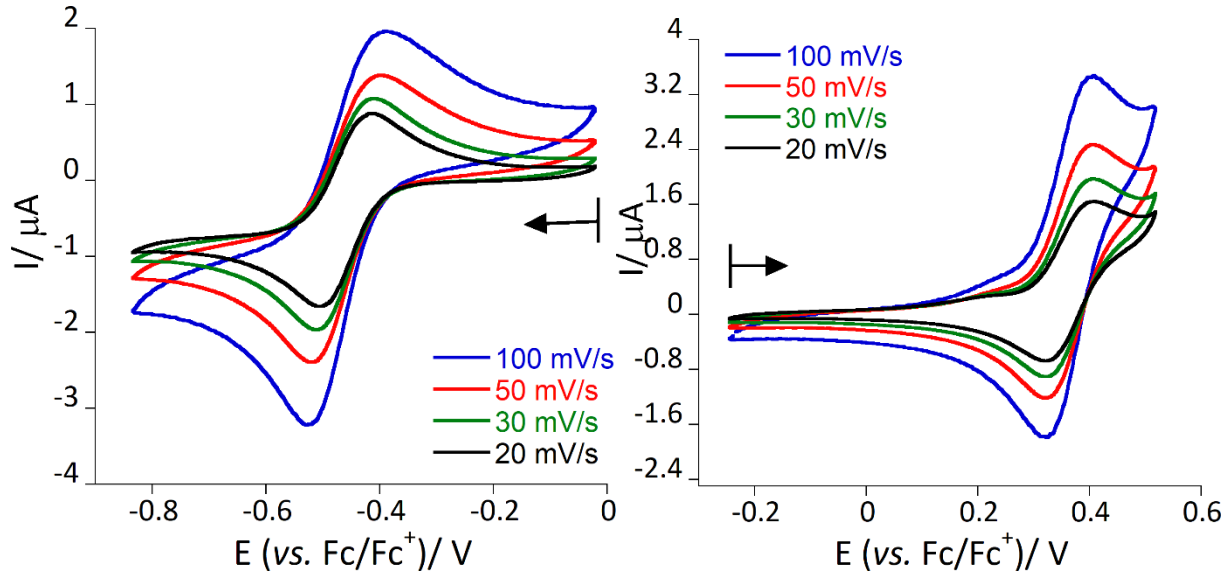

Fig. S41. Cyclic voltammograms for reduction (left) and oxidation (right) of **1** in 0.2 M (^{n}Bu$_4$N)PF$_6$ / MeCN with different scan rate. Arrow indicates the open circuit potential with the direction of the potential sweep.

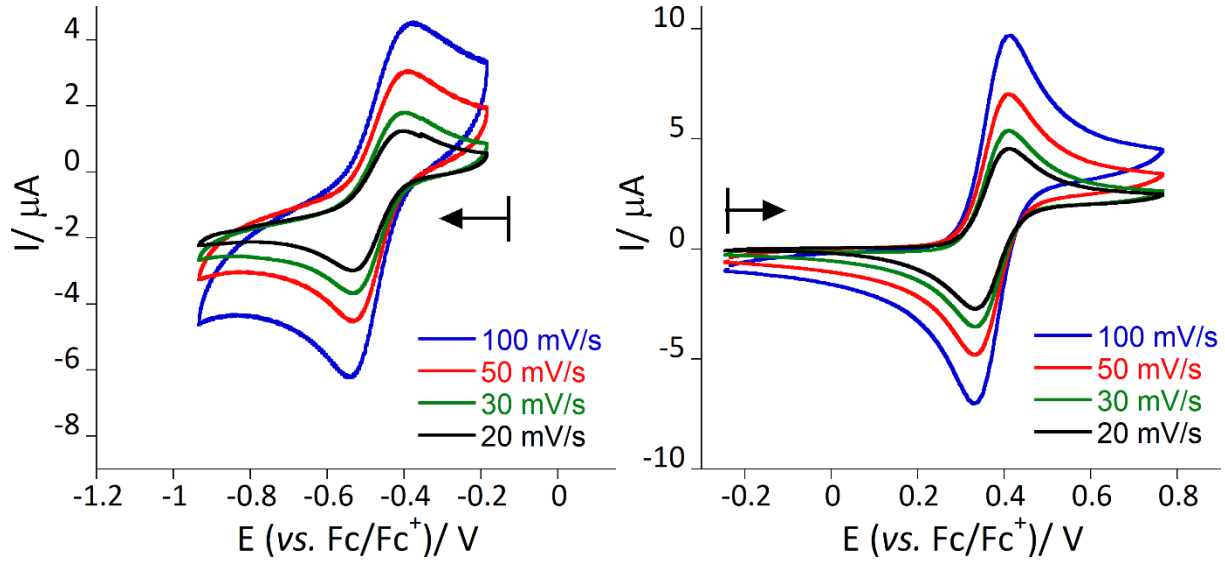

Fig. S42. Cyclic voltammograms for reduction (left) and oxidation (right) of **2** in 0.2 M (^{n}Bu$_4$N)PF$_6$ / MeCN with different scan rate. Arrow indicates the open circuit potential with the direction of the potential sweep.

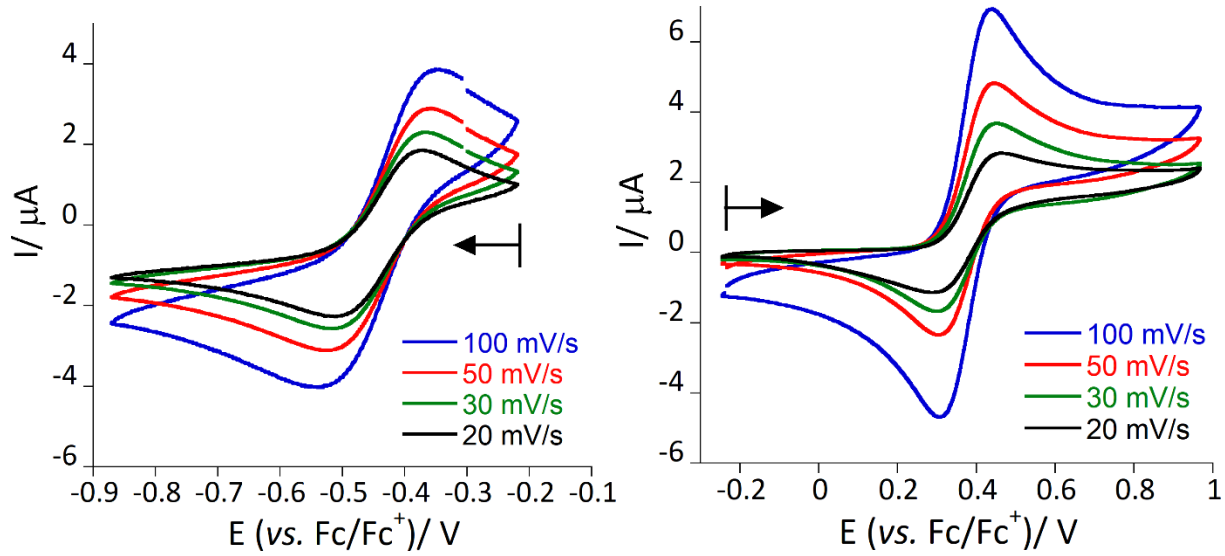

Fig. S43. Cyclic voltammograms for reduction (left) and oxidation (right) of **3** in 0.2 M (^{n}Bu$_4$N)PF$_6$ / MeCN with different scan rate. Arrow indicates the open circuit potential with the direction of the potential sweep.

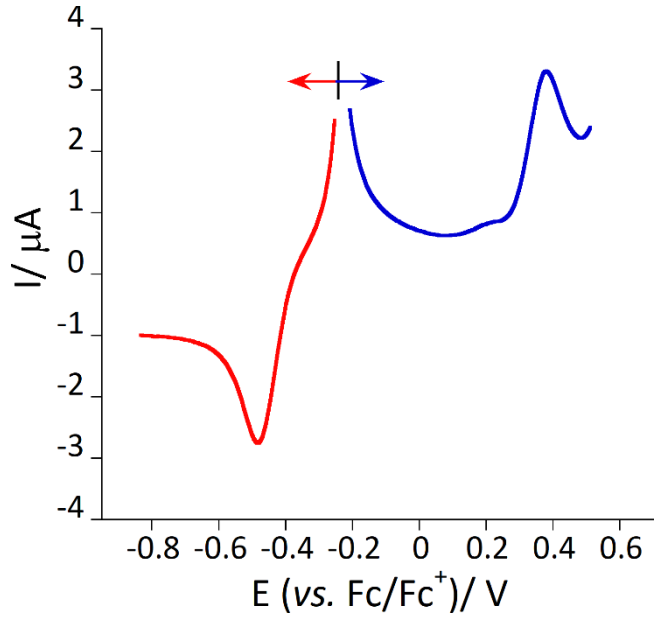

Fig. S44. Square wave voltammograms for **1** in 0.2 M (^{n}Bu$_4$N)PF$_6$ / MeCN. Arrows indicate the open circuit potential with the direction of the potential sweep.

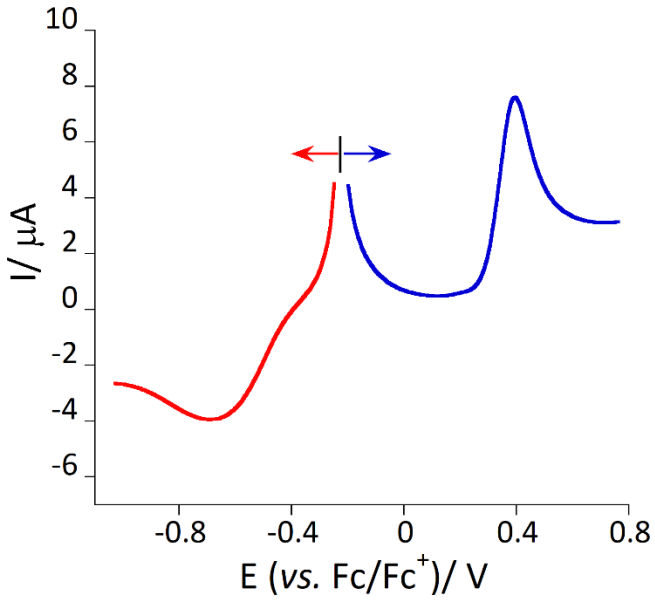

Fig. S45. Square wave voltammograms for **2** in 0.2 M (^{n}Bu$_4$N)PF$_6$ / MeCN. Arrow indicates the open circuit potential with the direction of the potential sweep.

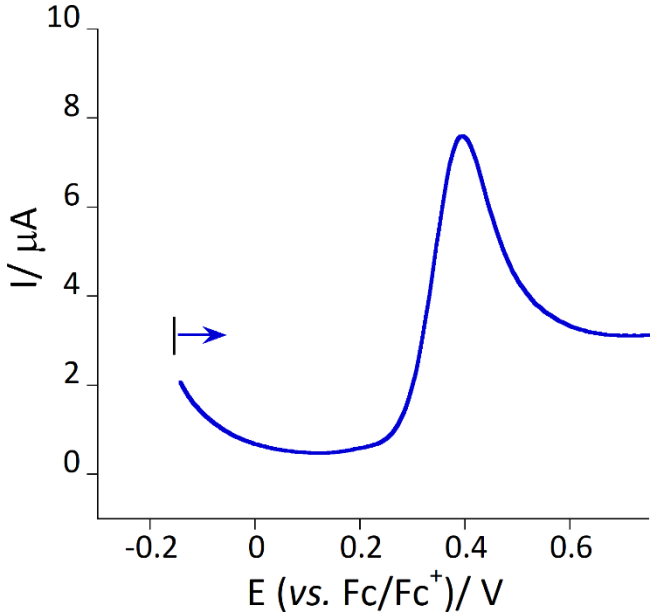

Fig. S46. Square wave voltammogram for oxidation of **3** in 0.2 M (^{n}Bu$_4$N)PF$_6$ / MeCN. Arrow indicates the open circuit potential with the direction of the potential sweep.

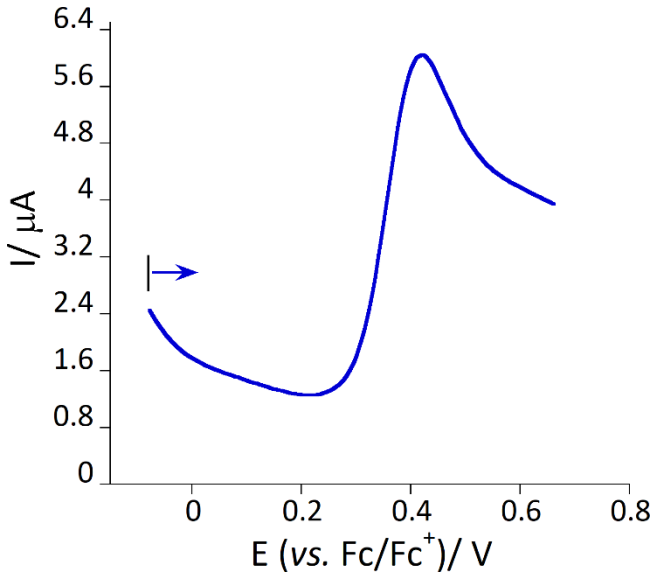

Fig. S47. Square wave voltammogram for **4** in 0.2 M (^{n}Bu$_4$N)PF$_6$ / MeCN. Arrow indicates the open circuit potential with the direction of the potential sweep.

Tables

Table S1. X-ray crystallography data for complexes **1** – **4**.

Complex		**1**	**2**	**3**	**4**
CCDC no	2098344	2098342	2098402	2098404	2098406
Temperature, K	240	100	100	100	100
Empirical formula	$C_{34}H_{36}N_8O_2ClMn$	$C_{34}H_{36}N_8O_2ClMn$	$C_{36}H_{39}N_9O_2BF_4Mn[+CH_3CN]$	$C_{38}H_{42}N_{10}O_2BF_4Mn$	$C_{38}H_{42}N_{10}O_2BF_4Mn$
Mol. Weight, g mol^{-1}	679.10	679.10	812.57	825.21	788.62
Crystal system	Monoclinic	Monoclinic	Monoclinic	Monoclinic	Orthorhombic
Space group	*P2/n*	*P2/n*	*$P2_1/n$*	*$P2_1/c$*	*Pccn*
a, Å	7.6419(2)	7.5907(2)	8.1393(4)	7.9902(4)	19.096(2)
b, Å	8.2294(2)	8.1774(2)	23.3849(10)	23.8380(13)	10.6565(14)
c, Å	25.7208(6)	25.5929(6)	20.7547(9)	20.9130(11)	17.243(2)
α, °	90	90	90	90	90
β, °	91.263(1)	90.0310(10)	101.029(3)	97.7740(10)	90
γ, °	90	90	90	90	90
V, $Å^3$	1617.14(7)	1588.61(7)	3877.4(3)	3946.7(4)	3508.8(8)
Z	2	2	4	4	4
d_{cal}, g cm^{-3}	1.395	1.420	1.322	1.389	1.493
μ, mm^{-1}	0.536	0.546	0.404	0.461	0.499
F(000)	708	708	1600	1720	1624
θ max	26.383	30.557	30.643	30.497	30.560
Completeness, %	99.8	99.8	98.8	99.3	99.2
Reflections collected	3313	4864	11835	11947	5341
Independent reflections	2912	3952	8349	9403	3706
Goodness-of-fit on F^2	1.169	1.035	1.025	1.038	1.026
Final R indices [$I>2\sigma(I)$]	R1 = 0.0509	R1 = 0.0362	R1 = 0.0610	R1 = 0.0535	R1 = 0.0400
	wR2 = 0.0974	wR2 = 0.0856	wR2 = 0.1532	wR2 = 0.1245	wR2 = 0.0867
Final R indices [all data]	R1 = 0.0608	R1 = 0.0496	R1 = 0.0899	R1 = 0.0713	R1 = 0.0708
	wR2 = 0.1010	wR2 = 0.0919	wR2 = 0.1707	wR2 = 0.1344	wR2 = 0.1004

$R1 = \sum||Fo| - |Fc||/\sum|Fo|$ and $wR2 = |\sum w(|Fo|^2 - |Fc|^2)|/\sum|w(Fo)^2|^{1/2}$

Table S2. Selected bond distances (Å) and bond angles (°) in **1**.

Complex	**1**	
	240 K	100 K
Mn(1)-N(1)	2.032(2)	2.0332(12)
Mn(1)-N(2)	1.988(2)	1.9854(12)
Mn(1)-O(1)	1.888(15)	1.8861(9)
N(1)-Mn(1)-N(2)	171.55(9)	171.87(5)
N(1)-Mn(1)-N(2)	90.08(8)	90.16(5)
N(1)-Mn(1)-O(1)	91.90(9)	91.74(5)
N(1)-Mn(1)-O(1)	84.73(8)	84.67(5)
N(2)-Mn(1)-O(1)	94.83(8)	94.77(4)
N(2)-Mn(1)-O(1)	88.26(8)	88.54(4)
N(1)-Mn(1)-N(1)	85.46(13)	85.59(7)
N(2)-Mn(1)-N(2)	95.22(12)	94.87(7)
O(1)-Mn(1)-O(1)	175.42(11)	175.11(6)

Table S3. Selected bond distances (Å) and bond angles (°) in **2** and **3** at 100 K.

Complex	**2**	**3**
Mn(1)-N(1)	2.218(2)	2.220(2)
Mn(1)-N(2)	2.240(2)	2.250(2)
Mn(1)-N(3)	2.108(2)	2.087(2)
Mn(1)-N(4)	2.095(2)	2.128(2)
Mn(1)-O(1)	1.8825(18)	1.8714(17)
Mn(1)-O(2)	1.8651(19)	1.8744(16)
N(1)-Mn(1)-N(2)	79.52(9)	79.54(7)
N(1)-Mn(1)-N(3)	162.23(9)	162.84(8)
N(1)-Mn(1)-N(4)	85.60(9)	84.29(7)
N(1)-Mn(1)-O(1)	87.53(8)	87.86(8)
N(1)-Mn(1)-O(2)	94.08(9)	93.69(7)
N(2)-Mn(1)-N(3)	84.09(9)	84.54(7)
N(2)-Mn(1)-N(4)	163.27(9)	161.60(8)
N(2)-Mn(1)-O(1)	94.84(9)	96.82(7)
N(2)-Mn(1)-O(2)	86.54(9)	86.03(7)
N(3)-Mn(1)-N(4)	111.50(9)	112.37(8)
N(3)-Mn(1)-O(1)	87.05(9)	87.71(8)
N(3)-Mn(1)-O(2)	91.72(9)	91.54(8)
N(4)-Mn(1)-O(1)	92.09(9)	91.24(8)
N(4)-Mn(1)-O(2)	86.94(9)	86.32(7)
O(1)-Mn(1)-O(2)	178.05(8)	176.96(7)

Table S4. Selected bond distances (Å) and bond angles (°) in **4** at 100 K.

Complex	**4**
Mn(1)-N(1)	2.2455(16)
Mn(1)-N(2)	2.0953(14)
Mn(1)-O(1)	1.8716(12)
N(1)-Mn(1)-N(2)	161.21(6)
N(1)-Mn(1)-N(2)	83.89(6)
N(1)-Mn(1)-O(1)	94.43(5)
N(1)-Mn(1)-O(1)	87.22(5)
N(2)-Mn(1)-O(1)	91.00(5)
N(2)-Mn(1)-O(1)	87.85(5)
N(1)-Mn(1)-N(1)	78.43(8)
N(2)-Mn(1)-N(2)	114.32(8)
O(1)-Mn(1)-O(1)	177.87(8)

Continuous Shape Measures (CShM) Analysis:

Continuous Shape Measures (CShM) analyses were carried out to determine the geometry around Mn ion. Based on the values obtained, the idealized polyhedron was matched with the actual coordination spheres. The smallest value is symbolic of the proximity of the actual coordination sphere and idealized polyhedron.

Table S5: CShM analysis data for complexes **1** – **4**.

Complex	Temp.	Structure				
		HP - 6	PPY - 6	**OC - 6**	TPR - 6	JPPY - 6
1	240 K	33.454	27.764	**0.386**	14.458	31.702
	100 K	33.351	27.892	**0.368**	14.632	31.892
2	100 K	32.280	23.059	**1.661**	10.329	25.821
3	100 K	31.966	22.526	**1.823**	9.952	25.238
4	100 K	32.285	22.299	**1.884**	9.999	25.148

HP – 6: Hexagon (D6h), PPY – 6 = Pentagonal pyramid, OC – 6: Octahedron (Oh), TPR – 6: Trigonal prism (D3h), JPPY – 6 = Johnson pentagonal pyramid J2 (C5v);

Octahedral Distortion Parameters[7]

$\sum$ is the sum of the deviation from 90° of the 12 *cis*-angles of the MnN_4O_2 octahedron; Θ is the sum of the deviation from 60° of the 24 trigonal angles of the projection of the MnN_4O_2 octahedron onto the trigonal faces; ζ is the distance distortion parameter, which is the sum of deviation from individual M-N/O bond distances to the mean metal-ligand bond distance.

Table S6 Selected Non-covalent cation-anion interactions parameters for **1** - **4** at 100 K.

Complex	Type of interaction	Distance
1	N-H···Cl	3.088 (1) Å
	C-H···Cl	3.524 (1) Å
		3.386 (2) Å
2	N-H···F(BF_4)	3.092 (1) Å
	N-H···N_{azo}	3.411 (2) Å
	π···π (between –PhN=NPh)	3.760 (1) Å
		3.691 (1) Å
	N=N···N=N	3.538 (2) Å
3	N-H···O(ClO_4)	3.099 (2) Å
	N-H···N_{azo}	3.438 (1) Å
	π···π (between –PhN=NPh)	3.589 (1) Å
	N=N···N=N	3.602 (1) Å
4	N-H···C(Ph)	3.703 (2) Å
	π···π (between –PhN=NPh)	4.301 (1) Å
	N=N···N=N	4.138 (3) Å

Table S7: Individual contributions to D-tensor for **1 - 4** calculated by CASSCF/NEVPT2.

1					**2**					**3**					**4**				
Block	Mult	Root	D	E	Block	Mult	Root	D	E	Block	Mult	Root	D	E	Block	Mult	Root	D	E
0	5	0	0.000	0.000	0	5	1	-0.027	-0.001	0	5	1	-0.027	-0.002	0	5	1	-0.030	-0.001
0	5	1	0.000	0.000	0	5	2	0.568	0.566	0	5	2	0.571	0.471	0	5	2	0.569	0.569
0	5	2	0.000	0.000	0	5	3	0.375	-0.375	0	5	3	0.372	-0.274	0	5	3	0.375	-0.376
0	5	3	0.000	0.000	0	5	4	0.012	0.011	0	5	4	0.007	0.006	0	5	4	0.013	0.013
0	5	4	0.000	0.000	1	3	0	4.230	0.008	1	3	0	3.985	0.007	1	3	0	3.770	0.010
1	3	1	4.850	5.263	1	3	1	-0.389	-0.388	1	3	1	-0.364	-0.244	1	3	1	-0.346	-0.346
1	3	2	1.746	-1.746	1	3	2	-0.222	0.279	1	3	2	-0.218	0.239	1	3	2	-0.202	0.264
1	3	3	-0.029	0.006	1	3	3	-0.001	-0.001	1	3	3	-0.000	-0.000	1	3	3	-0.001	-0.001
1	3	4	2.103	-2.103	1	3	4	-0.086	0.133	1	3	4	-0.075	0.112	1	3	4	-0.107	0.148
1	3	5	0.002	-0.002	1	3	5	-0.005	-0.006	1	3	5	0.027	-0.004	1	3	5	-0.010	-0.010
1	3	6	1.830	1.835	1	3	6	0.063	0.007	1	3	6	0.031	0.004	1	3	6	0.061	0.005
1	3	7	0.120	0.120	1	3	7	-0.036	-0.035	1	3	7	-0.042	-0.000	1	3	7	-0.041	-0.041
1	3	8	0.100	-0.100	1	3	8	-0.006	-0.006	1	3	8	0.003	-0.007	1	3	8	-0.004	-0.004
1	3	9	0.008	-0.008	1	3	9	-0.054	0.111	1	3	9	-0.070	0.072	1	3	9	0.139	0.086
1	3	10	-1.215	0.033	1	3	10	0.538	0.010	1	3	10	0.579	0.000	1	3	10	0.458	0.041
1	3	11	-0.730	0.028	1	3	11	-0.081	-0.081	1	3	11	-0.078	-0.076	1	3	11	-0.080	-0.080
1	3	12	0.033	-0.033	1	3	12	0.025	0.006	1	3	12	0.020	0.006	1	3	12	0.013	0.008
1	3	13	-0.928	0.029	1	3	13	0.747	0.029	1	3	13	0.741	0.028	1	3	13	0.776	0.018
1	3	14	0.019	-0.019	1	3	14	-0.001	-0.001	1	3	14	0.007	-0.001	1	3	14	-0.002	-0.002
1	3	15	0.014	0.016	1	3	15	-0.032	0.176	1	3	15	-0.114	0.209	1	3	15	-0.161	0.227
1	3	16	0.039	-0.039	1	3	16	-0.028	-0.028	1	3	16	-0.027	-0.025	1	3	16	-0.022	-0.022
1	3	17	0.016	-0.016	1	3	17	-0.073	0.081	1	3	17	-0.041	0.044	1	3	17	-0.033	0.039
1	3	18	0.022	0.032	1	3	18	-0.001	-0.001	1	3	18	-0.007	-0.004	1	3	18	-0.005	-0.005
1	3	19	0.000	0.000	1	3	19	0.017	0.004	1	3	19	-0.112	-0.076	1	3	19	0.020	0.002
1	3	20	0.021	-0.021	1	3	20	-0.392	-0.387	1	3	20	-0.187	-0.044	1	3	20	-0.393	-0.393
1	3	21	0.008	-0.008	1	3	21	-0.026	0.021	1	3	21	-0.074	-0.075	1	3	21	-0.031	0.031
1	3	22	0.017	0.017	1	3	22	-0.175	0.175	1	3	22	-0.186	0.045	1	3	22	-0.171	0.174
1	3	23	0.002	-0.002	1	3	23	-0.009	-0.009	1	3	23	-0.007	-0.006	1	3	23	-0.012	-0.012
1	3	24	0.044	0.056	1	3	24	-0.008	-0.008	1	3	24	-0.008	-0.008	1	3	24	-0.006	-0.006
1	3	25	0.019	-0.019	1	3	25	-0.014	0.019	1	3	25	-0.012	0.007	1	3	25	-0.010	0.014
1	3	26	0.002	-0.002	1	3	26	-0.001	0.002	1	3	26	-0.001	0.002	1	3	26	-0.001	0.002
1	3	27	0.019	0.020	1	3	27	-0.013	-0.013	1	3	27	-0.009	-0.006	1	3	27	-0.006	-0.006
1	3	28	0.064	-0.064	1	3	28	-0.007	-0.007	1	3	28	-0.007	-0.005	1	3	28	-0.007	-0.007
1	3	29	0.010	0.014	1	3	29	-0.000	-0.000	1	3	29	-0.000	-0.000	1	3	29	-0.000	-0.000

1	3	30	0.001	0.001	1	3	30	-0.012	0.013	1	3	30	-0.012	0.009	1	3	30	-0.014	0.015
1	3	31	0.000	0.001	1	3	31	-0.002	-0.002	1	3	31	-0.002	-0.000	1	3	31	-0.001	0.001
1	3	32	0.002	0.003	1	3	32	-0.002	0.002	1	3	32	-0.002	-0.002	1	3	32	-0.002	-0.002
1	3	33	0.000	-0.000	1	3	33	-0.020	-0.020	1	3	33	-0.021	-0.017	1	3	33	-0.022	-0.022
1	3	34	0.000	-0.000	1	3	34	0.003	0.000	1	3	34	0.003	-0.000	1	3	34	0.003	0.000
1	3	35	0.002	-0.002	1	3	35	0.001	0.000	1	3	35	0.001	0.000	1	3	35	0.001	0.000
1	3	36	0.001	0.001	1	3	36	-0.001	0.001	1	3	36	-0.001	0.001	1	3	36	-0.001	0.002
1	3	37	0.000	-0.000	1	3	37	-0.000	-0.000	1	3	37	-0.000	-0.000	1	3	37	-0.000	-0.000
1	3	38	0.000	-0.000	1	3	38	-0.001	0.001	1	3	38	-0.000	0.000	1	3	38	-0.001	0.001
1	3	39	0.001	-0.001	1	3	39	-0.000	-0.000	1	3	39	-0.000	-0.000	1	3	39	-0.000	-0.000
1	3	40	0.000	0.000	1	3	40	-0.003	-0.003	1	3	40	-0.003	-0.001	1	3	40	-0.003	-0.003
1	3	41	-0.000	0.000	1	3	41	0.000	0.000	1	3	41	0.000	0.000	1	3	41	0.000	0.000
1	3	42	0.000	-0.000	1	3	42	-0.000	-0.000	1	3	42	-0.000	0.000	1	3	42	-0.000	-0.000
1	3	43	0.004	0.005	1	3	43	-0.000	0.001	1	3	43	-0.001	0.001	1	3	43	-0.001	0.001
1	3	44	0.003	-0.003	1	3	44	0.045	0.000	1	3	44	0.044	0.000	1	3	44	0.044	0.000
2	1	0	1.204	-0.093	2	1	0	0.000	0.000	2	1	0	0.000	0.000	2	1	0	0.000	0.000
2	1	1	-0.143	0.143	2	1	1	0.000	0.000	2	1	1	0.000	0.000	2	1	1	0.000	0.000
2	1	2	-1.587	-1.698	2	1	2	0.000	0.000	2	1	2	0.000	0.000	2	1	2	0.000	0.000
2	1	3	-1.237	1.237	2	1	3	0.000	0.000	2	1	3	0.000	0.000	2	1	3	0.000	0.000
2	1	4	2.024	-0.015	2	1	4	0.000	0.000	2	1	4	0.000	0.000	2	1	4	0.000	0.000
2	1	5	4.815	-0.015	2	1	5	0.000	0.000	2	1	5	0.000	0.000	2	1	5	0.000	0.000
2	1	6	-0.704	0.704	2	1	6	0.000	0.000	2	1	6	0.000	0.000	2	1	6	0.000	0.000
2	1	7	-0.039	-0.120	2	1	7	0.000	0.000	2	1	7	0.000	0.000	2	1	7	0.000	0.000
2	1	8	-0.451	0.451	2	1	8	0.000	0.000	2	1	8	0.000	0.000	2	1	8	0.000	0.000
2	1	9	-0.791	-0.809	2	1	9	0.000	0.000	2	1	9	0.000	0.000	2	1	9	0.000	0.000
2	1	10	-0.219	0.219	2	1	10	0.000	0.000	2	1	10	0.000	0.000	2	1	10	0.000	0.000
2	1	11	-0.000	0.000	2	1	11	0.000	0.000	2	1	11	0.000	0.000	2	1	11	0.000	0.000
2	1	12	-0.171	-0.316	2	1	12	0.000	0.000	2	1	12	0.000	0.000	2	1	12	0.000	0.000
2	1	13	0.891	-0.006	2	1	13	0.000	0.000	2	1	13	0.000	0.000	2	1	13	0.000	0.000
2	1	14	-0.010	0.010	2	1	14	0.000	0.000	2	1	14	0.000	0.000	2	1	14	0.000	0.000
2	1	15	0.001	-0.000	2	1	15	0.000	0.000	2	1	15	0.000	0.000	2	1	15	0.000	0.000
2	1	16	-0.026	-0.026	2	1	16	0.000	0.000	2	1	16	0.000	0.000	2	1	16	0.000	0.000
2	1	17	-0.002	0.002	2	1	17	0.000	0.000	2	1	17	0.000	0.000	2	1	17	0.000	0.000
2	1	18	0.006	-0.003	2	1	18	0.000	0.000	2	1	18	0.000	0.000	2	1	18	0.000	0.000
2	1	19	-0.022	0.022	2	1	19	0.000	0.000	2	1	19	0.000	0.000	2	1	19	0.000	0.000
2	1	20	0.016	-0.002	2	1	20	0.000	0.000	2	1	20	0.000	0.000	2	1	20	0.000	0.000
2	1	21	-0.024	0.024	2	1	21	0.000	0.000	2	1	21	0.000	0.000	2	1	21	0.000	0.000
2	1	22	0.057	-0.000	2	1	22	0.000	0.000	2	1	22	0.000	0.000	2	1	22	0.000	0.000
2	1	23	-0.003	0.003	2	1	23	0.000	0.000	2	1	23	0.000	0.000	2	1	23	0.000	0.000
2	1	24	-0.005	-0.006	2	1	24	0.000	0.000	2	1	24	0.000	0.000	2	1	24	0.000	0.000

2	1	25	-0.017	-0.020	2	1	25	0.000	0.000	2	1	25	0.000	0.000	2	1	25	0.000	0.000
2	1	26	-0.013	0.013	2	1	26	0.000	0.000	2	1	26	0.000	0.000	2	1	26	0.000	0.000
2	1	27	0.063	-0.000	2	1	27	0.000	0.000	2	1	27	0.000	0.000	2	1	27	0.000	0.000
2	1	28	0.000	-0.000	2	1	28	0.000	0.000	2	1	28	0.000	0.000	2	1	28	0.000	0.000
2	1	29	-0.035	-0.039	2	1	29	0.000	0.000	2	1	29	0.000	0.000	2	1	29	0.000	0.000
2	1	30	-0.021	0.021	2	1	30	0.000	0.000	2	1	30	0.000	0.000	2	1	30	0.000	0.000
2	1	31	-0.012	0.012	2	1	31	0.000	0.000	2	1	31	0.000	0.000	2	1	31	0.000	0.000
2	1	32	-0.001	0.001	2	1	32	0.000	0.000	2	1	32	0.000	0.000	2	1	32	0.000	0.000
2	1	33	0.002	-0.000	2	1	33	0.000	0.000	2	1	33	0.000	0.000	2	1	33	0.000	0.000
2	1	34	-0.000	0.000	2	1	34	0.000	0.000	2	1	34	0.000	0.000	2	1	34	0.000	0.000
2	1	35	-0.004	0.004	2	1	35	0.000	0.000	2	1	35	0.000	0.000	2	1	35	0.000	0.000
2	1	36	-0.000	0.000	2	1	36	0.000	0.000	2	1	36	0.000	0.000	2	1	36	0.000	0.000
2	1	37	0.006	-0.001	2	1	37	0.000	0.000	2	1	37	0.000	0.000	2	1	37	0.000	0.000
2	1	38	-0.001	-0.002	2	1	38	0.000	0.000	2	1	38	0.000	0.000	2	1	38	0.000	0.000
2	1	39	-0.000	0.000	2	1	39	0.000	0.000	2	1	39	0.000	0.000	2	1	39	0.000	0.000
2	1	40	-0.000	0.000	2	1	40	0.000	0.000	2	1	40	0.000	0.000	2	1	40	0.000	0.000
2	1	41	0.004	-0.000	2	1	41	0.000	0.000	2	1	41	0.000	0.000	2	1	41	0.000	0.000
2	1	42	-0.000	-0.000	2	1	42	0.000	0.000	2	1	42	0.000	0.000	2	1	42	0.000	0.000
2	1	43	0.001	-0.000	2	1	43	0.000	0.000	2	1	43	0.000	0.000	2	1	43	0.000	0.000
2	1	44	-0.002	-0.003	2	1	44	0.000	0.000	2	1	44	0.000	0.000	2	1	44	0.000	0.000
2	1	45	-0.001	-0.001	2	1	45	0.000	0.000	2	1	45	0.000	0.000	2	1	45	0.000	0.000
2	1	46	-0.004	0.004	2	1	46	0.000	0.000	2	1	46	0.000	0.000	2	1	46	0.000	0.000
2	1	47	-0.000	-0.000	2	1	47	0.000	0.000	2	1	47	0.000	0.000	2	1	47	0.000	0.000
2	1	48	-0.000	0.000	2	1	48	0.000	0.000	2	1	48	0.000	0.000	2	1	48	0.000	0.000
2	1	49	0.003	-0.000	2	1	49	0.000	0.000	2	1	49	0.000	0.000	2	1	49	0.000	0.000

Table S8: The XYZ coordinates calculated by DFT

LS of $[Mn(5azo\text{-}sal_2\text{-}323)]^+$

Mn	5.68955858337724	5.35463839534209	6.39822444495277
O	4.59179994866975	5.38730443015562	7.93568806046120
N	4.42414846852885	3.99659461986987	5.60760572955936
N	4.59111782460234	6.86866243005620	5.54489614304606
N	2.63852624304001	0.77549249522603	11.65009365803513
N	2.72961508571529	0.77065382800451	10.41401834708413
C	3.81976203634195	3.11946495925321	7.78072140770854
C	3.33868004926233	1.98847753618487	8.45902820131686
H	3.07173721576034	1.09203004788967	7.89623276140193
C	4.13279267268377	4.29460021343967	8.51071736641475
C	3.80492067651717	3.13932602919022	6.32752093033040
C	5.37801521834017	8.11188157967270	5.70900675039436
C	3.92222862487272	4.29202340323575	9.91311785514482
H	4.14725987204027	5.20593240091938	10.46373475855660
C	3.19174544306592	1.98719576492164	9.83715669615565
C	4.04064415073645	4.10788369097932	4.19615522718343
H	3.38888087871799	3.26530367768170	3.92743842220272
H	4.93488566491210	4.05519670438267	3.56703340491687
C	2.16988986626337	-0.45151440625186	12.22273031030807
C	3.47766643976846	3.16237937623611	10.56443903488459
H	3.34142774954014	3.16984409292031	11.64513592068176
C	1.71336762338594	-1.54693915056525	11.47885550029283
H	1.69797511254106	-1.49393227478338	10.39123954197258
C	3.30678782146035	5.42462970067164	3.95733918907154
H	2.94169986048936	5.42414816617942	2.92089798750018
H	2.41707651109896	5.46681040536792	4.60432680220425
C	2.18323539931954	-0.50317757765326	13.61812372626127
H	2.53909247975048	0.36579773971690	14.17346964949287
C	4.14948406799731	6.67633507959361	4.14593134051059
H	5.05297288882166	6.62381031868731	3.52636647245588
H	3.57611008754660	7.56025166896167	3.82940638930434
C	1.27974397484103	-2.68969726072687	12.14314359648939
H	0.92112736486580	-3.54533826895995	11.56860462079587
C	1.75059883764100	-1.65308020227004	14.27761200264727
H	1.76508390170281	-1.69351522318864	15.36776682500680
C	1.29889834216505	-2.74730605901707	13.54060544235746
H	0.95709724822666	-3.64795939371794	14.05313617615780
H	3.14952155243807	2.41017595224345	5.83339877306293
H	3.76285135890260	6.93891832095882	6.13269902220233
H	4.74907086221665	9.00006255775273	5.55747556861695
H	6.15916017820904	8.11279392336986	4.93768801358447
O	6.78731549344514	5.38728464298381	4.86075930733530
N	6.95493887488595	3.99656397365370	7.18883919192073
N	6.78803326206926	6.86863507342675	7.25155837327495

N	8.74051324101764	0.77544563020184	1.14634561684524
N	8.64942040474377	0.77060564146414	2.38242058136994
C	7.55930891697273	3.11942892213390	5.01572111961937
C	8.04037561794894	1.98843610741071	4.33741244990310
H	8.30730223479896	1.09198263779627	4.90020603399299
C	7.24630217944714	4.29457257500296	4.28572816407670
C	7.57414851564725	3.13928456313711	6.46892152733326
C	6.00116284732008	8.11187196796844	7.08745376855461
C	7.45686131772990	4.29199305468327	2.88332694449574
H	7.23184155636983	5.20590563554695	2.33271138876884
C	8.18731111000410	1.98715469819479	2.95928419265487
C	7.33844803055036	4.10784049790581	8.60028951518535
H	7.99019286736324	3.26524503444584	8.86900274827163
H	6.44420698079756	4.05517175356259	9.22941286479220
C	9.20922707102596	-0.45153443237811	0.57371446565492
C	7.90140521382570	3.16234308675153	2.23200364817172
H	8.03763930993845	3.16980620806201	1.15130621137248
C	9.66580898349978	-1.54693106766903	1.31759415638585
H	9.68119616037021	-1.49391950054176	2.40520988753055
C	8.07233467224081	5.42456895625283	8.83910815077475
H	8.43742541440309	5.42407596740131	9.87554839433998
H	8.96204528116483	5.46673174886069	8.19211838659774
C	9.19588030235616	-0.50320613037530	-0.82167858939880
H	8.83997144885222	0.36574562306955	-1.37702819756718
C	7.22966574982842	6.67629340084899	8.65052172268458
H	6.32617739073941	6.62378697735862	9.27008875251493
H	7.80306022128532	7.56019621312286	8.96704806139639
C	10.09949628761286	-2.68966793367967	0.65331110770540
H	10.45815967258188	-3.54528680229902	1.22785387219240
C	9.62857898488040	-1.65308834566099	-1.48116176283201
H	9.61409322377649	-1.69353012553212	-2.57131631935600
C	10.08034462613004	-2.74728413009968	-0.74415048998996
H	10.42219503988105	-3.64792100033413	-1.25667726578234
H	8.22953244638517	2.41011946116547	6.96304170135880
H	7.61630038542962	6.93887536943201	6.66375454157931
H	6.63012641233834	9.00003868648525	7.23898902074456
H	5.22001806396490	8.11279766830895	7.85877268479897

HS of $[Mn(5azo\text{-}sal_2\text{-}323)]^+$

Mn	5.68955974926262	5.20194196453756	6.39822480462501
O	4.83022532822679	5.19187271074595	8.05649063291204
N	4.11129704644934	3.98487851570616	5.68092565729337
N	4.48438780371156	6.91735227769713	5.62431143587849
N	2.60160011067857	0.68492677333747	11.75511642378308
N	2.55693066605658	0.74536881030264	10.51850602994032
C	3.68032192573483	3.07734619841429	7.88313164500706

C	3.11061799098825	1.99160068132387	8.56520579772447
H	2.60232971850711	1.20645548284959	8.00252273936137
C	4.30460649807927	4.11370596557206	8.62130925124845
C	3.47613214189149	3.18240712785837	6.44382952200323
C	5.32782122399314	8.12077043207596	5.73180334429969
C	4.33275689511708	4.01458351458029	10.03250440444089
H	4.80401139860104	4.82399887953132	10.59078330463090
C	3.16919346936753	1.89790344045759	9.94736639393316
C	3.63532861378685	4.17400820582843	4.30845505500463
H	2.90221212472890	3.39244959884904	4.06163471647147
H	4.48320091758493	4.07531182563740	3.62097448239782
C	1.97461590887105	-0.47131209310077	12.32369971761064
C	3.78639792193679	2.92822667521757	10.68379018346583
H	3.82315052081037	2.86476437560886	11.77055749985893
C	1.32181902706511	-1.46280441663227	11.58010228620619
H	1.27171444889013	-1.38135487892707	10.49535423577239
C	2.98999703297721	5.55047726109820	4.15283246039903
H	2.52901146447237	5.58868477796527	3.15583700727964
H	2.16852658914930	5.64722696027095	4.88010972195526
C	2.04248584318165	-0.56307653535161	13.71528356004801
H	2.55524158262530	0.22392703311029	14.27009531661648
C	3.92878962169424	6.74380636637160	4.26753980941148
H	4.77581290226855	6.62517824254383	3.57952964305508
H	3.38920483916700	7.65777550876629	3.97219863211057
C	0.74270108355796	-2.54075067995315	12.24129401977294
H	0.23198762526161	-3.31561500066650	11.66721408552080
C	1.46051379981484	-1.64695228577387	14.37185035942096
H	1.51436377758359	-1.71794196790480	15.45916208243629
C	0.81013002356682	-2.63629181753602	13.63535025419299
H	0.35234708920519	-3.48535030713116	14.14548068133336
H	2.68273380337195	2.55284281389119	6.01667154871095
H	3.71018216121747	7.01016343869642	6.27734857199630
H	4.73211399870290	9.03886082138655	5.61767206275230
H	6.05586869728592	8.09266187379524	4.90910448238261
O	6.54889340659531	5.19184181889812	4.73995878390852
N	7.26778435006295	3.98483135824645	7.11552602789010
N	6.89478637712174	6.91731702128360	7.17213303922984
N	8.77732725985298	0.68479134580353	1.04134606183750
N	8.82200794413524	0.74523885976750	2.27795571215978
C	7.69873144893526	3.07728043411499	4.91332247374462
C	8.26840030008964	1.99151505338384	4.23125068773131
H	8.77665993135632	1.20635287315064	4.79393587878054
C	7.07448059967440	4.11365853088241	4.17514238344153
C	7.90292446917440	3.18233841694475	6.35262418128907
C	6.05139139165344	8.12076159044222	7.06463712489476
C	7.04631868028386	4.01452951217299	2.76394795200570

H	6.57508233347419	4.82395432741401	2.20566748266362
C	8.20981318828787	1.89781170275323	2.84909098030346
C	7.74375936909111	4.17395005946420	8.48799606117925
H	8.47685079345150	3.39236861945077	8.73481866331669
H	6.89588412010884	4.07528300389785	9.17547702654438
C	9.40446700279717	-0.47135774010133	0.47275159588870
C	7.59263911997610	2.92815160091291	2.11266504298737
H	7.55586964949567	2.86467993318728	1.02589884155329
C	10.05738925067416	-1.46277451507534	1.21633967572344
H	10.10749299060102	-1.38132333849140	2.30108767825243
C	8.38913507036033	5.55039897087898	8.64361444864578
H	8.85012250564299	5.58859442934816	9.64060955420994
H	9.21060802868201	5.64712053100973	7.91633630921764
C	9.33658298381028	-0.56313282143717	-0.91883077381536
H	8.82372100744539	0.22380716282055	-1.47363452543871
C	7.45038030550837	6.74375757326427	8.52890463594101
H	6.60335401128711	6.62515829475175	9.21691604014872
H	7.98999434256480	7.65771043921229	8.82424271833469
C	10.63662134119087	-2.54065437347637	0.55513973689931
H	11.14743046703162	-3.31546094645098	1.12921252728054
C	9.91866803077483	-1.64694293977562	-1.57540566731958
H	9.86480537824345	-1.71794192958053	-2.66271615920729
C	10.56918147883341	-2.63620447391494	-0.83891536586721
H	11.02705300354559	-3.48521135277017	-1.34905216562114
H	8.69630338813388	2.55275067662091	6.77978368194723
H	7.66899448152766	7.01010080897333	6.51909474304894
H	6.64712761126466	9.03883361931247	7.17876477972578
H	5.32334320181581	8.09267929165971	7.88733626327876

LS of [Mn(5azo-sal$_2$-323)]Cl

Mn	5.68807112186435	5.35423504018891	6.38992958528722
O	4.62642268868948	5.37572260151204	7.95089856547184
N	4.41638034153018	3.99378630193642	5.61528178603564
N	4.59095393110758	6.86091072767397	5.54263590423537
N	2.62075497942553	0.78624749301432	11.66362329110467
N	2.71159677931247	0.78170914645426	10.42745287754593
C	3.82067528775831	3.12021196152859	7.79305530566618
C	3.32770883813194	1.99492781151150	8.47230418527096
H	3.04440663782543	1.10363532127524	7.90925503722294
C	4.15573517591061	4.28928066531976	8.52356416314913
C	3.79789480207606	3.14041560299933	6.34021359306086
C	5.37904103047363	8.10330627568048	5.68967208875508
C	3.95384370445723	4.28562554910356	9.92799773092091
H	4.19567340572702	5.19497173453116	10.47906666357586
C	3.18842342381291	1.99229736465734	9.85121783851566
C	4.02711547099728	4.10036155957904	4.20521915183945

H	3.37318967283735	3.25742512958973	3.94247837392790
H	4.91872923573708	4.04395401357979	3.57266176234295
C	2.13742872534566	-0.43578246547876	12.23466597210700
C	3.49657544451901	3.16155862370374	10.57950298826874
H	3.36732645637527	3.16852311891134	11.66107117312713
C	1.66961518579156	-1.52558132236166	11.48951712656865
H	1.65638832549193	-1.47175263999472	10.40191445230102
C	3.29420021792425	5.41720122547433	3.96654799421164
H	2.92294470157554	5.41348126139528	2.93214120940596
H	2.41038547058869	5.46387113202754	4.62020483449379
C	2.14840726987428	-0.48870811632117	13.62999394882570
H	2.51322626627008	0.37580587449782	14.18648390498686
C	4.14035136739843	6.66798173513543	4.14846793771159
H	5.03405750067690	6.61837222111829	3.51401548724796
H	3.55923488476912	7.55068572412148	3.84046318326478
C	1.22250818830038	-2.66392239606111	12.15237771471299
H	0.85513259058985	-3.51508770461878	11.57673401991202
C	1.70217368968092	-1.63418511627510	14.28811258938092
H	1.71485680842338	-1.67562518810942	15.37824238748909
C	1.23926802868949	-2.72280428928634	13.54981595411077
H	0.88689712210305	-3.61995117142430	14.06131335593067
H	3.13705990718461	2.41305883449294	5.85059563503524
H	3.74658983111857	6.97180967281679	6.11912439095428
H	4.74339690794156	8.98860923326763	5.54433251008420
H	6.15413600523202	8.10966045600025	4.91173432466998
O	6.77510311588428	5.37989328686629	4.84059261242744
N	6.96961056402271	3.99665441655669	7.17146417824722
N	6.79912223629088	6.86827680860998	7.22682551808134
N	8.75605060881807	0.77815149447144	1.12703526309315
N	8.65809262378895	0.77195328759747	2.36261154281932
C	7.56100835478656	3.11672704886901	4.99628333517682
C	8.04606685992653	1.98802131350373	4.31732903536109
H	8.32292689349842	1.09473876109714	4.88043236506051
C	7.23609858459459	4.28891392865275	4.26626713784274
C	7.58651771307441	3.14004164740079	6.44932004092620
C	6.01263996729896	8.11161169561104	7.06333217434783
C	7.43796178703065	4.28385050768129	2.86205725583871
H	7.20275186888279	5.19484584570486	2.31084008481404
C	8.18689291651601	1.98504357914861	2.93849724415800
C	7.36502329091142	4.11217735578212	8.57903743883516
H	8.02103809920049	3.27181487138953	8.84484674965083
H	6.47670872099251	4.06022525450356	9.21648044512372
C	9.23543946494744	-0.44568443002359	0.55649616251765
C	7.88732199185046	3.15647920936044	2.21040551597670
H	8.01705837846468	3.16272554389842	1.12888967554634
C	9.69211644734104	-1.53975242679458	1.30231185571250

H	9.69847189444726	-1.48836540481820	2.39009012912696
C	8.09937581749756	5.43070193679415	8.80711718555028
H	8.47401258070864	5.43404601485962	9.84017874362489
H	8.98320232490057	5.47114013138032	8.15187031478888
C	9.23340186467697	-0.49547475321276	-0.83898171704499
H	8.87715465171813	0.37231076809553	-1.39592764603595
C	7.25479829075654	6.68168525221530	8.62149073955938
H	6.35782530281496	6.63189083848287	9.25056700797135
H	7.83191606786992	7.56653923628075	8.92883074785224
C	10.13738911354271	-2.67905911903545	0.63989288699581
H	10.49620318828122	-3.53352332749340	1.21604802562164
C	9.67771136472119	-1.64194381225403	-1.49668173004055
H	9.67214735973110	-1.68089607225398	-2.58696204582016
C	10.12976902919353	-2.73468838572380	-0.75776165917124
H	10.48076078708132	-3.63256976287943	-1.26891985265882
H	8.24923337695798	2.41479836976421	6.93975915969709
H	7.62102313902535	6.93331079783202	6.62966208891851
H	6.64381795185134	8.99951978049266	7.20809143818056
H	5.23569322397134	8.11493665938166	7.83870344045275
Cl	1.76060175859084	7.73032884903764	6.95204811214366

HS of [Mn(5azo-sal$_2$-323)]Cl

Mn	5.73890144921374	5.19910160471390	6.36819176675263
O	4.89021871047151	5.15281623911997	8.03803006570989
N	4.14724118008924	3.91528524386280	5.65712863032791
N	4.50063016131192	6.82505388548099	5.63647594007766
N	2.56744188756856	0.72396055537998	11.77130874731894
N	2.51633298323164	0.77985510199955	10.53447362431266
C	3.69211229017280	3.06000016798104	7.87523556257960
C	3.09849977915398	1.99570254622365	8.56983057611787
H	2.57224494503389	1.21666116430186	8.01502479247048
C	4.34065555610987	4.08973968351402	8.60371281313968
C	3.49439655942839	3.14099251140388	6.43123887793215
C	5.26424235953757	8.08024689153557	5.77090103849521
C	4.36759165847951	4.00001726794533	10.01666719535301
H	4.85788094031044	4.80378835792705	10.56682576031297
C	3.15473752121137	1.91215700524870	9.95330346690737
C	3.68318378363009	4.08509357701027	4.28044335618722
H	2.95100643127441	3.30255265248522	4.03114699753969
H	4.53721993735394	3.98125893493589	3.60080999049155
C	1.91364152976804	-0.41265788266244	12.34921539260314
C	3.79688713768938	2.93383652935033	10.67979000598211
H	3.83329238274546	2.88028256350843	11.76712397774070
C	1.22924989713919	-1.38941508160970	11.61462644870446
H	1.17399616610816	-1.31123704916024	10.52989623430587
C	3.03938422396428	5.46083229281190	4.11430427946961

H	2.60851607266584	5.50754778500799	3.10405925618066
H	2.19910017479592	5.54903714329895	4.81930532982092
C	1.98866554742995	-0.50065695376986	13.74069590853219
H	2.52632094929962	0.27446595151299	14.28863109576009
C	3.96501577294838	6.66136311221860	4.26828616781546
H	4.81808934807594	6.57619824019771	3.58280763612851
H	3.41016271729552	7.57243303654356	3.99236529041071
C	0.62574695468604	-2.44851670875651	12.28445670389207
H	0.09037655530129	-3.21167102715608	11.71720508664603
C	1.38222112202446	-1.56563413459406	14.40596872710285
H	1.44183371861874	-1.63348614811824	15.49318229220500
C	0.70016487291262	-2.54009710444462	13.67837368144158
H	0.22317562544027	-3.37429403554166	14.19536029338039
H	2.69173026403804	2.51373647031288	6.01582607505637
H	3.69931681402570	6.88426924907481	6.27577417856190
H	4.59847717366963	8.95161622491930	5.67681803955140
H	5.99226815065236	8.12722246074740	4.94856698992726
O	6.59276609064423	5.21400076253555	4.70371553682004
N	7.30185519746144	4.01682308162778	7.06993293903049
N	6.90739893972655	6.96460157390572	7.18570426366163
N	8.80897668395046	0.71047220757310	0.99790693938153
N	8.85827315159960	0.76987308808101	2.23441982324196
C	7.73837392339123	3.10107272495797	4.87142574469120
C	8.30786885768255	2.01431071500621	4.18987915397593
H	8.81029731313188	1.22561981796984	4.75281207154342
C	7.12056033241587	4.14187757050551	4.13429235389498
C	7.93736996493962	3.21053602316503	6.30898416200786
C	5.98620579725340	8.10853556892545	7.10515261518109
C	7.10113635144360	4.04913958505358	2.72206786274475
H	6.63567232372228	4.86201370300594	2.16407723314869
C	8.25336317308790	1.92504080930424	2.80771430553864
C	7.77811642514874	4.20872364556953	8.44421827629947
H	8.51456970787719	3.42845436394348	8.68343444699394
H	6.93189791160677	4.10101270246251	9.13167634708749
C	9.42600615526730	-0.44931638057875	0.42606681681194
C	7.64511747590733	2.96184415909842	2.07147220483706
H	7.61336946623874	2.90109333718147	0.98438726408811
C	10.07391315636049	-1.44649865831962	1.16622977361741
H	10.12882406130299	-1.36641932268546	2.25085404628183
C	8.42040515854334	5.58575229539819	8.61186647990650
H	8.89712387852265	5.60578907964028	9.60201482973089
H	9.23048629778500	5.69807507190199	7.87410933253657
C	9.35183062457846	-0.53927999114415	-0.96529270610077
H	8.84287004224410	0.25217476070715	-1.51724936159574
C	7.47447811729367	6.77666271380560	8.53230844976388
H	6.63499865332550	6.63444264170977	9.22519858444660

H	8.00951552141744	7.68795626483461	8.84547070335733
C	10.64160354587977	-2.52849191167704	0.50177424320291
H	11.14828196533061	-3.30800369398255	1.07310072590777
C	9.92239442269749	-1.62716799251071	-1.62511031863642
H	9.86344472048871	-1.69682120494595	-2.71223188663069
C	10.56771077040177	-2.62231598904296	-0.89204276208776
H	11.01641176541200	-3.47467146340725	-1.40470607141420
H	8.72866516583377	2.58357229964469	6.74235167145209
H	7.67101714406571	7.11835730936003	6.53243345842641
H	6.51245677852744	9.06651365364723	7.23632884545429
H	5.26030384115438	8.01219355158117	7.92435155002868
Cl	1.76073482145972	7.37063320142997	7.39988375812588

Table S9. The structural parameters and energies for the low-spin (LS) and high-spin (HS) states for molecular geometries of **1** calculated by ωB97M-D4.

	[Mn(5azo-sal$_2$-323)]$^+$ of **1**			[Mn(5azo-sal$_2$-323)]Cl of **1**		
Structural parameters	LS	MECP	HS	LS	MECP	HS
Mn-N_{amine}[a]	2.056	2.141	2.235	2.047	2.121	2.171
Mn-N_{amine}	2.056	2.141	2.235	2.056	2.156	2.270
Mn-N_{imine}	2.018	2.084	2.118	2.017	2.076	2.082
Mn-N_{imine}	2.018	2.084	2.118	2.024	2.098	2.165
Mn-O	1.889	1.877	1.868	1.888	1.877	1.871
Mn-O	1.889	1.877	1.868	1.893	1.879	1.874
N_{amine}-H				1.028	1.027	1.027
Cl···H				2.283	2.291	2.293
Spin transition energetics between the LS and HS states (LS↔HS)						
ΔE_{el}	1.381 kcal/mol			1.684 kcal/mol		
ΔE_{el+ZPE}	-0.522 kcal/mol			-0.105 kcal/mol		

[a] nitrogen atom involved in N-H···Cl hydrogen bond.

References

1. M. Tripathi, C. G. Giri, D. Das, R. Pande, S. Sarkar, S. Giri, G. Roymahapatra and A. Sarkar, *Nucleosides Nucleotides Nucleic Acids*, 2018, **37**, 563-584.
2. T. Degen, M. Sadki, E. Bron, U. König and G. Nénert, *Powder Diffr.*, 2014, **29**, S13-S18.
3. G. M. Sheldrick, SADABS Version 2.03, Bruker Analytical X-Ray Systems, Madison, WI, USA, 2000.
4. Farrugia, L. WinGX and ORTEP for Windows: an update. *J. Appl. Crystallogr.* 2012, **45**, 849-854.
5. O. V. Dolomanov, L. J. Bourhis, R. J. Gildea, J. A. K. Howard and H. Puschmann, *J. Appl. Crystallogr.*, 2009, **42**, 339-341.
6. C. F. Macrae, P. R. Edgington, P. McCabe, E. Pidcock, G. P. Shields, R. Taylor, M. Towler and J. van de Streek, *J. Appl. Crystallogr.*, 2006, **39**, 453-457.
7. R. Ketkaew, Y. Tantirungrotechai, P. Harding, G. Chastanet, P. Guionneau, M. Marchivie and D. J. Harding, *Dalton Trans.*, 2021, **50**, 1086-1096.